COLUMBIA | SIPA
Center for Environmental Economics and Policy

CEEP Working Paper Series
Working Paper Number 19

October 2021

Environmental Drivers of Agricultural Productivity Growth: CO_2 Fertilization of US Field Crops

Charles A. Taylor and Wolfram Schlenker

https://ceep.columbia.edu/sites/default/files/content/papers/n19.pdf

Environmental Drivers of Agricultural Productivity Growth: CO_2 Fertilization of US Field Crops

Charles A. Taylor[1] and Wolfram Schlenker[1,2]

September 2021

Abstract

We assess the CO_2 fertilization effect on US agriculture using spatially-varying CO_2 data from NASA's Orbiting Carbon Observatory-2 (OCO-2) satellite covering the majority of US cropland under actual growing conditions. This study complements the many CO_2 enrichment experiments that have found important interactions between CO_2 and local environmental conditions in controlled settings. We use three empirical strategies: (i) a panel of CO_2 anomalies and county yields, (ii) a panel of spatial first-differences between neighboring counties, and (iii) a cross-sectional spatial first-difference. We find consistently high fertilization effects: a 1 ppm increase in CO_2 equates to a 0.5%, 0.6%, and 0.8% yield increase for corn, soybeans, and wheat, respectively. Viewed retrospectively, 10%, 30%, and 40% of each crop's yield improvements since 1940 are attributable to rising CO_2.

Acknowledgments: This work was supported by the U.S. Department of Energy, Office of Science, Biological and Environmental Research Program, Earth and Environmental Systems Modeling, MultiSector Dynamics, Contract No. DE-SC0016162.

[1] School of International and Public Affairs, Columbia University, 420 West 118th St., New York, NY 10027.

[2] National Bureau of Economic Research (NBER), 1050 Massachusetts Ave., Cambridge, MA 02138.

Introduction

The Green Revolution has significantly increased agricultural yields around the world. In the United States, the agricultural sector had one of the highest productivity growth rates in the post-war period (Jorgenson and Gollop 1992) with input usage, mechanization, irrigation, and improved crop genetics all being identified as drivers of yield growth (Wang, Heisey, Schimmelpfennig, and Ball 2015). Growth in agricultural productivity is not confined to the agricultural sector itself: the adoption of high-yield varieties in India had significant positive economic spillovers for the larger economy (Gollin, Hansen, and Wingender 2021). Understanding the drivers of agricultural productivity growth is hence important for economic growth both inside the agricultural sector as well as other sectors.

Corn yields in the US, for example, have increased six-fold since 1940, prior to which point they were rather flat, as shown in Figure 1. Similarly, yields of US soybeans and winter wheat have increased by a factor of three since 1940. At the same time, atmospheric CO_2 has been steadily increasing, which has driven a global greening trend: over the last 40 years, half of global vegetated area has undergone greening as defined by growing season integrated leaf area index, of which 70% is attributed to elevated CO_2 (Zhu et al. 2016). How much has elevated CO_2 contributed to the observed increase in crop yields during this time? Establishing a causal link between two trending variables is statistically challenging. Industrialization, both in agriculture and other sectors, might have independently increased CO_2 levels as well as yields. Disentangling the effect of CO_2 fertilization from other productivity drivers is difficult given that CO_2 has risen smoothly in tandem with other factors like mechanization and average crop yields.

Field experiments and process-based analyses have been the most common approaches to attribute yield trends. These approaches, however, face challenges of their own. The conditions in a well-controlled experiment might not be indicative of real-world farming conditions. There are large regional differences in crop responses to CO_2 that reflect geographic variation in crop distribution and environmental conditions (McGrath and Lobell 2013). CO_2 fertilization may be negligible in the presence of limiting factors like nutrient deficiency (Kimball et al. 2001, Hungate, Dukes, Shaw, Luo, and Field 2003, Reich et al. 2006, Ziska and Bunce 2007), while it is generally higher under water deficit conditions (Ottman et al. 2001, Leakey, Uribelarrea, Ainsworth, Naidu, Rogers, Ort, and Long 2006, Keenan, Hollinger, Bohrer, Dragoni, Munger, Schmid, and Richardson 2013, Morgan et al. 2011), although some have found a larger effect under irrigation (Zheng, He, Guo, Hao, Cheng, Li, Peng, and Xu 2020). Elevated CO_2 may increase high temperature stress due to stomatal

closure (Batts, Morison, Ellis, Hadley, and Wheeler 1997). A decline in the global carbon fertilization effect over time has been documented, likely attributable to changes in nutrient and water availability (Wang et al. 2020). While CO_2 enrichment experiments, both in the laboratory and field, have generated important insights into the physiological channels of the fertilization effect and its environmental interactions, they are limited in the extent to which they reflect real-world growing conditions in commercial farms at a large geographic scale.

To this end, we provide a new approach to estimating the effect of CO_2 on crop yields that relies neither on process-based models nor localized field experiments. While experiments are conducted at individual sites, our dataset covers the majority of the US crop growing area. We use observed ambient CO_2 data from NASA's recently-launched Orbiting Carbon Observatory-2 (OCO-2) satellite and county-level crop yield data. The OCO-2 satellite detects changing ambient CO_2 concentrations that occur within and across locations and growing seasons (Crisp 2015). We focus on the US, which is the biggest producer of corn and soybeans, accounting for 33% of global production (FAOSTAT) over OCO-2's sample timeframe from 2015-2020, and 7% of global wheat production.

While gaseous CO_2 ultimately diffuses across space and becomes uniformly distributed in the atmosphere,[1] this process occurs over the course of weeks to months and is affected by specific emission events, local CO_2 sources and sinks, as well as wind and weather dynamics (Hakkarainen, Ialongo, and Tamminen 2016). Variations in satellite CO_2 readings around the steady upward trend are driven by such local disturbances. We link the resulting variation (i.e., anomalies) to fluctuations in yields. Since OCO-2 measures the entire air column, we replicate all of our analyses using modelled data from NOAA's CarbonTracker, which provides spatially-resolved estimates of surface-level CO_2 from 2000 to 2018.

We document a significant CO_2 fertilization effect for corn, soybeans, and winter wheat using three separate approaches that isolate both time-series and cross-sectional variation with both OCO-2 and CarbonTracker data. Our results are robust to a myriad of sensitivity checks, i.e., the functional form (logarithmic versus levels), whether the temporal trend is common to all counties or varies by state or county, whether or not we include controls for co-occurring air pollutants, weather, or vegetative greenness measures. The latter two factors are designed to absorb local feedback effects, i.e., a situation where elevated CO_2 is a response to a crop-failure that reduces photosynthetic activity, which would only downward

[1]The spatial diffusion of CO_2 is what makes climate change a global public goods problem. It also allows scientists to rely on singular sources of long-term CO_2 measurements, like the Mauna Loa Observatory, to estimate global CO_2 levels, which are then incorporated into global process-based models.

bias our estimates.

In the US, we find fertilization effects that are high relative to the literature: a 1 part per million (ppm) increase in CO_2 equates to a 0.5%, 0.6%, and 0.8% yield increase for corn, soybeans, and wheat, respectively. Our findings are relevant in several contexts: first, in providing an example of how satellite-based measures of CO_2 can complement field experiments to ensure external validity of the effect of CO_2 on agriculture and ecosystem functioning at a large scale. Second, our finding that 10-40% of historical crop yield improvements in the US are attributable to CO_2 fertilization has implications for the literature on the drivers of agricultural productivity, which can have very large economic spillovers (Gollin et al. 2021).

Lastly, while our paper focuses on explaining past drivers of productivity growth, it has also implications for the future: future CO_2 fertilization effects are critical to accurately estimating the impact of climate change on agriculture. Our preferred panel specification has been used to link random year-to-year weather fluctuations to annual yield outcomes (Schlenker and Roberts 2009). The effects are clearly visible in Figure 1 where we see a significant reduction in national corn yields in 2012 when the Corn Belt experienced higher than normal extreme heat. Studies employing such panel variation to estimate climate change damages relate outcomes of interest to random exogenous year-to-year weather fluctuations to obtain damage estimates (Dell, Jones, and Olken 2014). Overall, climate change is predicted to increase the occurrence of extreme heat and significantly reduce yield potential. This approach, which relies on annual variation in weather, does not take into account longer-term dynamics which are correlated with climate change. Part of the estimated damages may be offset by yield gains from rising CO_2.

There is a gap between process-based studies of climate change which incorporate CO_2 fertilization and statistical ones which tend to omit it (Lobell and Asseng 2017), and the resulting estimates of climate impacts can vary greatly. For example, one study found that the significant negative net welfare effects on agriculture in the absence of CO_2 fertilization become negligible with fertilization (Moore, Baldos, and Hertel 2017). Others argue that crop responses to CO_2 are now understood well enough for fertilization estimates to be directly included in global climate models and impact projections (Toreti et al. 2020). Our paper demonstrates that increases in CO_2 can also have strong countervailing fertilization effects, at least at current levels. Given that experimental evidence shows a tapering of the CO_2 fertilization effect at higher levels, a linear extrapolation into the future has to be considered with caution.

Background

Plants respond directly to rising CO_2 through photosynthesis and stomatal conductance, which is the basis for the fertilization effect (Long, Ainsworth, Rogers, and Ort 2004, Ainsworth and Rogers 2007). The process varies by crop type. For C3 crops like soybeans, wheat, and rice, mesophyll cells containing ribulose-1,5-bisphosphate carboxylase-oxygenase (RuBisCO) are in direct contact with the air. RuBisCO is an enzyme that fixes atmospheric CO_2 during photosynthesis and in oxygenation of the resulting compound during photorespiration. Thus, higher ambient CO_2 increases photosynthetic CO_2 uptake because RuBisCO is not CO_2-saturated at today's atmospheric levels (Long et al. 2004). For C4 crops like corn, on the other hand, RuBisCO is located in bundle sheath cells where CO_2 levels are several times higher than atmospheric levels. At this concentration, RuBisCO is CO_2-saturated and there may not be a direct photosynthetic response to changing atmospheric CO_2 levels. However, C4 yields are still indirectly affected through increased water use efficiency via reduction in stomatal conductance (Long, Ainsworth, Leakey, Nösberger, and Ort 2006). All things being equal, one would expect a larger CO_2 fertilization effect for wheat and soybeans than for corn.

Historical estimates of yield responses to CO_2 have relied on experiments in greenhouses and laboratory controlled-environments where CO_2 levels can easily be controlled. An early survey concluded that doubling ambient CO_2 increased yields by 24 to 43% for C3 crops in the context of full water and nutrient availability (Kimball 1983), which aligned with USDA reporting a 33% increase in yields for most crops under similar settings (Allen Jr., Baker, and Boote 1996). In recent decades, free-air concentration enrichment (FACE), a process involving a series of pipes in fields emitting CO_2-enriched air, has allowed for larger-scale trials in more realistic crop growing conditions. A survey of over 25 years of FACE experiments concludes that increasing CO_2 from 353 to 550 ppm results in 19% higher C3 yields, on average, while C4 crops were only affected under conditions of water scarcity (Kimball 2016). FACE experiments tend to show a lower CO_2 fertilization effect than either laboratory or greenhouse enclosure studies (Long et al. 2006). FACE-derived estimates have been found to generally align with assumptions in global crop model simulations (Tubiello et al. 2007). We also note recent work that utilized OCO-2 satellite data estimate the impact of the 2019 Midwestern floods on CO_2 uptake and crop productivity (Yin et al. 2020).

Data

Measurements of atmospheric CO_2 come from the Orbiting Carbon Observatory-2 (OCO-2). Launched in 2014, OCO-2 is NASA's first satellite designed specifically to measure atmospheric CO_2 with the goal of better understanding the geographic distribution of CO_2 sources and sinks and their changes over time. We downloaded version B10206 of the bias-corrected OCO-2 LITE Level 2 product, specifically the 'XCO2' value of averaged dry air CO_2 mole fraction over the atmospheric column between the ground and the satellite. While the satellite measures the entire column, as long as the ground level disturbance is not systematically correlated with disturbances in higher altitudes, we will get an unbiased estimate of ground-level conditions. A typical daily output contains over 150,000 XCO2 global readings, including the latitude-longitude point. Readings have quality flags (about 50% of readings), which we exclude from our analysis.

NOAA's CarbonTracker provides spatially-resolved estimates of ground-level CO_2 from 2000 to 2018 derived from measurements of air samples collected at 460 sites around the world by 55 laboratories. Unconnected to OCO-2, CarbonTracker involves an inverse model of atmospheric CO_2 that adjusts surface-level CO_2 uptake and releases to align with observational constraints. We use use product release CT2019B (Jacobson et al. 2020) and the level 1 estimates which correspond to 25m above the Earth's surface.

We seasonally adjust CO_2 levels from OCO-2 and CarbonTracker to account for annual patterns in which ambient concentrations decrease in the spring and summer when plants are actively photosynthesizing and increase in the fall and winter when plants are respiring on net. To identify CO_2 anomalies relative to this seasonality pattern, we estimate the average seasonality over the contiguous US with a 4^{th}-order Chebychev Polynomial over the year which we normalize to [-1,1] by transforming January 1st to equal -1 and December 31st to equal 1 with leap years having an additional day as well. We restrict the seasonality so the value on January 1 (time -1) equals the value on December 31 (time 1).

The left chart of Figure A1 displays the seasonality in CO_2 in the OCO-2 data. We include a time trend to account for the annual increase in CO_2. Our seasonality adjusted values factor out the seasonality and re-normalize all values to July 1^{st}. Note that in the construction of the 4^{th}-order Chebyshev polynomial we include all non-flagged readings over the US, not just those over cropland. We assign each seasonally adjusted OCO-2 reading to the PRISM grid (1/24° grid in latitude and longitude) in which it falls. Readings are averaged if there are more than one for a grid during the growing season from April to September. The PRISM grids within a county are then averaged using the amount of cropland area in

the PRISM grid, where we aggregate the 30m-resolution from USDA's Cropland Data Layer to the PRISM grid. An analogous procedure is used for CarbonTracker, where we take the distance-weighted average of the surrounding four CarbonTracker grids for each PRISM grid to derive PRISM-grid level CO_2 exposure, which is then aggregated to the county level using cropland weights from the Cropland Data Layer. Figure A7 displays the cross-plot of CO_2 anomalies from the OCO-2 satellite and CarbonTracker during the four years (2015-2018) in which the datasets overlap.

Figures A2, A3, and A4 display the resulting number of observations per county and by crop that have both CO_2 readings and annual yield data over the six years from 2015 to 2020 for OCO-2 (top panel) and from 2000 to 2018 for CarbonTracker (bottom panel). Since we include both county fixed effects and county-specific time trends, we need at least three degrees of freedom per county, i.e., we can only include counties with at least 3 observations in our regressions.

Solar-induced chlorophyll fluorescence (SIF) is another remote sensing product available from the OCO-2 satellite. SIF is a measure of terrestrial photosynthesis that captures the energy emitted from plant chlorophyll molecules immediately following light absorption between wavelengths 600-800nm (Baker 2008). The OCO-2 SIF retrieval is based on in-filling solar Fraunhofer lines around 757nm and 771nm which limit the impact of atmospheric scattering due to aerosols or thin clouds lines (Sun, Frankenberg, Jung, Joiner, Guanter, Köhler, and Magney 2018). As with XCO2, we use bias-corrected SIF retrievals from the LITE Level 2 product. This SIF product opens new opportunities for improved mechanistic understanding of the response of crop yields to climate change and environmental conditions (Guan, Berry, Zhang, Joiner, Guanter, Badgley, and Lobell 2016). We adjust for SIF seasonality in the same way as we do for CO_2, as shown in the right chart of Figure A1.

Enhanced Vegetation Index (EVI) comes from NASA's MODIS Terra Vegetation satellite product MOD13Q1v006, which is generated every 16 days at 250m resolution. EVI is used to minimize canopy background variation, maintain sensitivity over dense vegetation, and remove residual atmosphere contamination caused by smoke and sub-pixel thin cloud clouds (Didan 2015). Values are averages over the growing season window from April to September over NLCD cropland area at 30m resolution for each county.

For weather we use daily fine-scale PRISM data at 2.5 minute resolution, or 4.5 km by 4.5 km, following the approach from Schlenker and Roberts (2009) which found that four weather variables (two temperature, two precipitation) predict yields well. The two temperature variables are degree days 10-29°C (moderate degree days) and degree days

above 29°C (extreme degree days) for corn. The upper bound is slightly higher for soybeans, resulting in degree days 10-30°C and degree days above 30°C. We use the same degree days variables for winter wheat as for soybeans. We experimented with using separate temperature measures by trimester (Tack, Barkley, and Nalley 2015), but did not find an improved fit. In each regression we also include a quadratic of season-total precipitation. Precipitation and degree days are summed across the six-month growing season from April to September and spatially averaged using the same PRISM grid weights that are aggregates of USDA's Cropland Data Layer for each county.

County-level crop yields for corn, soybeans, and winter wheat were obtained from USDA's National Agricultural Statistics Service.

Model

We utilize data from the OCO-2 satellite and CarbonTracker to estimate the CO_2 fertilization effect on corn, soybeans, and wheat in the US, the world's biggest agricultural producer. We focus on counties east of the Rocky Mountains (excluding Florida), an area accounting for the vast majority of US production of corn and soybeans, but for completeness we also replicate the analyses across the entire continental US as well as the primarily-rainfed area east of the 100° meridian that were used in previous studies (Schlenker and Roberts 2009). We match the yield data with local CO_2 readings and weather outcomes over the area where corn, soybeans, and winter wheat are grown within each county, respectively. All models use log of county-level yields as the outcome variable and seasonality-adjusted CO_2 in ppm unless otherwise noted.

We employ three modelling approaches that exploit differing sources of variation to identify the CO_2 fertilization effect: first, a panel model that effectively links CO_2 and yields anomalies. These anomalies are calculated after controlling for the four weather variables that were found to best predict corn and soybean yields (Schlenker and Roberts 2009) and criteria air pollutants (CO, NO_2, O_3, PM_{10}, SO_2). The panel model includes county fixed effects to account for differences in average yields across counties driven by factors such as soil quality and average climate, as well as county-specific time trends to account for local trends.

Our panel model specification is:

$$y_{it} = \alpha_{i0} + \alpha_{i1}t + \beta\ CO_{2it} + \boldsymbol{\gamma}\mathbf{W}_{it} + \boldsymbol{\delta}\mathbf{P}_{it} + \epsilon_{it} \tag{1}$$

where y_{it} is log crop yield in county i in year t; α_{i0} is a county fixed effect; α_{i1} is a county-specific time trend; β measures the observed CO_2 fertilization effect from the seasonally-adjusted CO_2 reading (CO_{2it}) in the county i in year t; $\boldsymbol{\gamma}$ is a control vector for weather (two temperature degree day variables, precipitation and precipitation-squared), while $\boldsymbol{\delta}$ is a control for five criteria air pollutants P_{it} (CO, NO_2, O_3, PM_{10}, SO_2). We use the daily mean for CO, NO_2, PM_{10}, and SO_2, and a restricted cubic spline with seven knots for O_3 (Boone, Schlenker, and Siikamäki 2019). Finally, ϵ_{it} are the errors (clustered at the state level to account for spatial correlation).

Second, we employ a spatial first difference model (SFD - Residuals) that is a generalization of Druckenmiller and Hsiang (2019). It compares the change in the CO_2 and yield anomalies across neighboring counties after removing county fixed effects and county-specific time trends in a given year, while again controlling for spatial differences in the other control variables (weather and other pollutants). To do this, we use a two step procedure: we first derive anomalies by factoring out fixed effects and county-specific time trends for all variables:

$$v_{it} = \alpha_{i0} + \alpha_{i1} t + \epsilon_{it} \tag{2}$$

where $v_{it} \in \{y_{it}, CO_{2it}, \mathbf{W}_{it}, \mathbf{P}_{it}\}$ to obtain the anomalies $\epsilon_{it}^{(v)}$ for each variable. By the Frisch-Waugh-Lovell theorem, regressing $\epsilon_{it}^{(y)}$ on $\epsilon_{it}^{(CO_2)}$ while controlling for $\epsilon_{it}^{(\mathbf{W})}$ and $\epsilon_{it}^{(\mathbf{P})}$ would give the same estimate for β as in equation (1). Instead, we look at the spatial first difference by pairing each county i with all of its neighbors j, defined as having a common coordinate in the county shape file. We take the difference in anomalies in a given year between neighbors: $\Delta_{ijt}^{(v)} = \epsilon_{it}^{(v)} - \epsilon_{jt}^{(v)}$, so any common shock would be differenced out. In a second step we then link these differences in annual anomalies (one observation for each county-pair per year):

$$\Delta_{ijt}^{(y)} = \beta \Delta_{ijt}^{(CO_2)} + \boldsymbol{\gamma} \Delta_{ijt}^{(\mathbf{W})} + \boldsymbol{\delta} \Delta_{ijt}^{(\mathbf{P})} + \epsilon_{ijt} \tag{3}$$

Third, we use a the SFD cross-sectional model to examine persistent average gradients in CO_2 and yields in space while again controlling for weather and co-pollutants. Ignoring annual anomalies (shocks), for each variable we derive the average outcome over all years $\overline{v_i} = \frac{1}{T} \sum_{t=1}^{T} v_{it}$, and again pair county i to all its neighbors j, defined as having a common coordinate in the county shape file. We take the difference in average outcomes between neighbors: $\Delta_{ij}^{(v)} = \overline{v_i} - \overline{v_j}$ and link these differences in space in a cross-sectional regression

(one observation for each county-pair):

$$\Delta_{ij}^{(y)} = \beta \Delta_{ij}^{(CO_2)} + \boldsymbol{\gamma} \Delta_{ij}^{(\mathbf{W})} + \boldsymbol{\delta} \Delta_{ij}^{(\mathbf{P})} + \epsilon_{ij} \tag{4}$$

The latter two SFD methods address concerns about the high spatial correlation in CO_2 levels. Different setups require different assumptions, i.e., that the annual CO_2 anomalies are uncorrelated with other omitted explanatory variables or that the average gradient in CO_2 is uncorrelated with other omitted explanatory variables. The fact that we obtain a robust consistent positive CO_2 fertilization effect makes it less likely that they are driven by the particular assumptions of each individual approach.

We illustrate our identification strategies in Figure 2. For the panel model, the top row shows CO_2 anomalies as measured by OCO-2 and CarbonTracker and how they relate to yield anomalies in an example year 2015. Note that in our actual panel regressions we include additional years. Figure A5 illustrates the variation in the panel model another way, highlighting the correlation for one particular county in Iowa over time after controlling for the trend. The bottom row in Figure 2 shows how gradients of CO_2 and yield anomalies are calculated across neighbors in an example latitude band in Iowa for the SFD-residual model. Note that in our SFD regressions we include as observations all neighboring gradients and not just horizontal ones, as well as all counties in the US and not just Iowa.

For each of these three modelling approaches, we provide estimates using CO_2 data from both the OCO-2 satellite and CarbonTracker. This provides different spatial coverage in sampled counties and temporal span (2015-2020 for OCO-2 and 2000-2018 for CarbonTracker). CarbonTracker has an advantage of explicitly modelling surface-level CO_2, while OCO-2 readings are column-averaged. On the other hand, OCO-2 are raw measurements from a satellite, while CarbonTracker is a reanalysis product that might suffer from promulgation of interpolation errors.

Results

Figure 3 shows our main results of the aggregate effect of CO_2 on county-level crop yields in the US. The point estimates of the CO_2 fertilization effect are positive in all cases, and significant for 15 of the 18 regressions. A 1 ppm increase in CO_2 equates to yield increases for corn, soybeans, and wheat of 0.5%, 0.6%, 0.8%, respectively, using our preferred panel model specification with OCO-2 data from 2015 to 2020 (green line in coefficient plot). In this case, the fertilization effect is less for corn (C4 crop) and greater for soybeans and winter wheat (C3

crops), as observed in controlled experiments. However, the corn estimate becomes larger when using the modelled CarbonTracker data that spans a longer timeline (2000-2018) and larger geographic extent. For soybeans and winter wheat, alternating between OCO-2 and CarbonTracker also increases the point estimates, but generally does not produce statistically different estimates. Figure A7 plots the correlation between OCO-2 and CarbonTracker anomalies during the four years (2015-2018) in which the datasets overlap. The regression coefficients from our preferred panel models are shown in columns (a) and (c) of Table A1. Results do not appear to be driven by outliers: Figure A6 plots the anomalies for both OCO-2 and CarbonTracker in the preferred panel model after the covariates are factored out with the regression line and a 90% confidence band.

Many factors influence yields beyond CO_2, and to that end we see that much variation remains after accounting for CO_2 as well as our controls for weather and other environmental factors. However, as long as CO_2 fluctuations are uncorrelated with the other remaining unaccounted factors, our approach provides an unbiased estimate of the CO_2 fertilization effect. Moreover, as we show below, the inclusion and exclusion of a myriad of controls known to influence crop yields do not significantly alter our findings, so any omitted variable would have to be correlated with both CO_2 and yields, but not the other controls. In addition, the SFD models, which allow us to directly isolate variation between neighboring counties, both for annual shocks and for average levels, consistently give positive coefficients. This provides additional assurance that the results are not driven by annual effects at the regional level or through feedback loops.

We perform a number of sensitivity checks that produce largely similar results. First, we vary the model specification: our baseline model links log yields to CO_2 levels, assuming that a 1 ppm change in CO_2 has the same *relative* (percent) effect on yields. Figure A8 links log yields to log CO_2 levels assuming a constant elasticity, Figure A9 links yields to CO_2 levels, assuming that a 1 ppm change in CO_2 has the same *absolute* effect on yields, while for completeness Figure A10 links yields to log CO_2. Results are very similar. The one minor difference is that the larger CO_2 fertilization effects found for corn using the CarbonTracker data in our main analysis are reduced somewhat when the dependent variable is yields instead of log yields.

Second, we vary the time trends to allow for the possibility that temporal patterns in CO_2 levels and crop yields may be occurring at a geographic level different than the county level—e.g., state-level policies may drive energy or agricultural production. Results are largely similar using state trends (Figure A11), but become less precise when trends

are excluded altogether (Figure A12), highlighting our approach to not correlate trending variables. In other words, the granularity of the time trend (state-specific versus county-specific) does not matter, as long a trend is included to account for the steady increase in global CO_2.

Third, we run our analyses comprising different US geographies as visualized by the colored regions in Figures A2-A4. Similar results are shown using the entire contiguous US in Figure A13 and the primarily-rainfed agricultural counties east of 100° meridian in Figure A14—mitigating concerns the this relationship is driven by regional dynamics like irrigation.

Fourth, we add a control for vegetation intensity in order to rule out endogenous feedback effects, e.g., where crop photosynthesis influences the ambient CO_2, rather than the other way around (Yin et al. 2020). It is important to note that such a feedback would downward bias our results, yet we find larger estimates to begin with. Figure A15 controls for solar-induced florescence (SIF) derived from OCO-2, as well as the Enhanced Vegetation Index (EVI) from MODIS in the case of the longer duration CarbonTracker data. Omitting the four weather variables in these regressions, we find that the inclusion of such vegetation measures increases the observed CO_2 coefficients for corn and soybeans to some extent, but not wheat. We would expect this local feedback to be stronger in corn and soybean-growing counties in our sample, where the combined cropland area in the 2018 Census was 47% and 49% of county land area, respectively. The combined cropland area in the counties growing winter wheat in our sample is only 35%, i.e., crops cover a smaller fraction of the overall county area. The negative bias is likely the result of adverse local weather conditions reducing yields and photosynthesis, thereby increasing observed CO_2 readings, leading to a negative correlation between yields and CO_2. We note that this specification has limitations given that vegetation measures like SIF and EVI have been used to directly model crop yields. Nevertheless, the coefficient remains significant in almost all cases even after accounting for greenness measures.

Alternatively, Figure A16 only uses CO_2 measures at the beginning of the growing season (April-June) to further limit potential plant growth-CO_2 feedbacks. The sample size is reduced in half when using OCO-2 data as the satellite only provides readings for a subset of locations during each orbit and we limit the time frame to three months instead of six months. Accordingly, the standard errors increase significantly and the estimates become noisier, although not statistically different. CarbonTracker, on the other hand, is reanalysis data and does not suffer from the same issue: the number of observations is the same

irrespective of which months we include as they are consistently available for each grid. The point estimates and confidence intervals hardly change at all. We therefore attribute the fluctuations of the estimates in the revised OCO-2 sample to the reduction in observations rather than a systematic difference in crop response to CO_2 during the early part of the growing season.

Fifth, we show in Figure A17 that our results are robust to omitting controls for other pollutants, which we include in our main specification to address concerns that the fossil fuel usage driving the increase in atmospheric CO_2 is also associated with co-occurring pollutants like ozone, nitrogen oxide, and sulfur dioxide, each of which has been shown to affect crop yields (Boone et al. 2019, Sanders and Barreca 2021).

Finally, we test for potential economic confounders, e.g., if local CO_2 anomalies are driven by a change in energy use, which in turn is driven by economic activity. In such a case, it is plausible that the higher yields we attribute to a CO_2 fertilization effect may actually reflect different farming practices when the local economy is strong and farmers invest more in their crop (i.e., apply more fertilizer). The SFD analyses should address these concerns by comparing differences in CO_2 and yield anomalies across county neighbors, given that neighboring counties generally face similar economic conditions. As additional evidence, Table A2 regresses aggregate US log yields on GDP growth rates (i.e., change in log GDP). We find no evidence that yields are linked to overall economic conditions in the US.

Relatedly, one may be concerned that our results are influenced by the degree of urban intensity, which can affect the proportion of land in agriculture, industrial pollution, or other things that may be correlated with CO_2. To address this, Table A1 includes an interaction of our CO_2 measure with each county's urban-rural continuum level (1-6 values) as categorized by USDA. We find a very imprecisely estimated crop fertilization effect in the most urban counties, which agrees with the near absence of cropland in these places. However, among all other county classifications, we find a CO_2 fertilization effect of generally similar magnitude, implying that the effect is not limited to places that are relatively more or less rural. This also mitigates concerns of a reverse feedback: that higher aggregate photosynthesis activity in counties with majority cropland (i.e., generally more rural) can act as a CO_2 sink that drives variation in observed local CO_2 levels.

Discussion

Global ambient CO_2 has increased by 2 to 2.5 ppm per year, on average, or 0.5% annually since 2000. Our results imply that CO_2 fertilization may have been a large contributor to recent crop productivity in the US. Our baseline estimates of yield responses of 0.5% to 0.8% per 1 ppm CO_2 are on the very high end of the range found in the literature—put another way, yields may have increased 1-2% per year due to CO_2 fertilization in recent years. Looking historically since 1940, corn yields have increased by 500% and soybeans and winter wheat yields by 200% as shown in Figure 1. During this time ambient CO_2 levels increased by slightly more than 100 ppm. A back-of-the-envelope calculation using our present-day estimates implies that CO_2 fertilization is responsible for increasing yields by 50% for corn, 60% for soybeans, and 80% for wheat—or about 10%, 30%, and 40% of past productivity growth for each crop, respectively.

The choice of using a logarithmic or linear extrapolation becomes crucial when projecting out yield responses to a doubling of CO_2. Figures A8-A10 variously log-transform the independent variable (CO_2) and the dependent variable (crop yield) and find similar magnitude results when concentrating on the observed range of CO_2 values in 2000-2020. While this is unsurprising as they give similar linearized local approximations, we urge caution in the forward project of our results.

Most contemporary estimates of CO_2 fertilization are derived from free-air concentration enrichment (FACE) experiments, in which CO_2 levels were raised by 190 to 200 ppm, on average, over a baseline average of 350 ppm. Surveying past FACE results, this 54-57% increase over the baseline (or 19% log difference) in CO_2 is associated with average yield increases of 18-19% (Kimball 2016, Ainsworth and Long 2021). However, this average effect conceals significant variation in the yield response across crops, location, and growing conditions. A FACE study of dryland wheat in Australia, for example, showed that a 40% increase in CO_2 was associated with yield increases of 24% and 53% in two sites, with some yield responses reaching 79% (Fitzgerald et al. 2016). Under varying environmental conditions, equivalent yield responses above 35% have been observed for corn, rice, cotton, as well as various leguminous and root crops (Kimball 2016, Ainsworth and Long 2021). It is worth noting that a strong positive relationship between CO_2 and yields should not be inherently surprising. CO_2 is a purchased input in many agricultural settings. The gas has long been pumped into greenhouses to spur photosynthesis and increase the yield of horticultural crops. Optimal CO_2 concentrations of 900 ppm have been suggested, which is over twice current ambient levels (Mortensen 1987).

Nevertheless, we offer some potential explanations for why our CO_2 fertilization estimates are higher than the average found in the literature. First, our study looks only at small increases in CO_2, and it may be inappropriate to extrapolate out fertilization effects which may diminish at higher CO_2 levels. As noted, most studies (including FACE, open top chamber, and greenhouse experiments) involve large one-time increases in CO_2 levels of 200 ppm or more over ambient levels. In contrast, our paper relies on variation in the range of 13 ppm during the OCO-2 timeline from 2015 to 2020 and 39 ppm for CarbonTracker from 2000 to 2018. Such marginal increases could produce relatively higher fertilization effects given the diminishing photosynthetic response curve of plants to elevated CO_2. The rate of CO_2 assimilation in C4 plants, for example, is close to saturated at CO_2 concentrations of 400 ppm (Lambers and Oliveira 2019). Our results may reflect higher yield responses around current ambient CO_2 levels that occur at a steeper part of the photosynthetic response curve. This same dynamic could explain part of the observed decline in the global carbon fertilization effect over time (Wang et al. 2020).

Another consideration is that CO_2 concentrations in FACE studies fluctuate widely due to air turbulence (Kimball 2016). When elevated CO_2 is supplied in cycles or pulses, crop responses may be lower than if the CO_2 is supplied more steadily (Bunce 2012). Just as CO_2 levels can be better controlled in chamber studies than FACE experiments, it is also possible that the smaller absolute variation in ambient CO_2 utilized in our study results in less fluctuations as well.

It is worth noting that there are only two large-scale and long-standing FACE experiments in the US that focus on agriculture: one in Maricopa, AZ, and another at the University of Illinois in Champaign, IL (Ainsworth and Long 2021). Other FACE experiments study non-cropland ecosystems like forests, grasslands, and tundra, as well as crop responses in other countries. Only the Champaign site has the potential to approximate agricultural conditions in the Midwest, where most crop production occurs in the US. Thus it is possible that FACE experiments do not fully reflect the growing conditions and farming practices of the major growing regions. Given the important CO_2 interactions with nutrient availability (Kimball et al. 2001, Hungate et al. 2003, Reich et al. 2006, Ziska and Bunce 2007) and water availability (Ottman et al. 2001, Leakey et al. 2006, Keenan et al. 2013, Morgan et al. 2011, Zheng et al. 2020), as well as nutrient-water-CO_2 interactions (Markelz, Strellner, and Leakey 2011), CO_2 fertilization effects could vary between FACE experiments and commercial agricultural operations in response to differing fertilization and input regimes, soil and water management practices, and local air pollution and climate anomalies across

regions—as well as conditions that vary over time. Our experimental design utilizing OCO-2 satellite measures of ambient CO_2 allows us to account for this variation at a larger scale and across multiple years of observations.

Conclusion

We find a significant and robust CO_2 fertilization effect by linking OCO-2 satellite-measured CO_2 fluctuations to yield fluctuations of corn, soybeans, and winter wheat from 2015 to 2020. For additional verification, we obtain generally similar results using modelled ground-level CO_2 data from CarbonTracker from 2000-2018. Our study spans more than half of the commercially-farmed area of these crops in the US and offers a test of whether the fertilization effects found in controlled experiments can be verified under real-world growing conditions. While panel models linking weather and yield anomalies have shown the possible detrimental effect of extreme heat on yield, the same setup can be used to show that localized CO_2 anomalies drive significant yield changes—outcomes also reflected when utilizing alternate empirical approaches like spatial first differences across neighboring counties using both annual anomalies as well as average CO_2 gradients in space. Our preferred panel specification suggests that 10%, 30%, and 40% of observed yield gains for corn, soybeans, and wheat, respectively, since 1940 are due to increases in CO_2, an important driver of agricultural productivity growth.

Our paper shows how satellite-based measures of CO_2 can be useful in complementing FACE field experiments, especially in the context of ensuring the external validity of estimates of the effect of CO_2 on agriculture and ecosystem functioning at a large scale. The approach can be extended to study real-world crop responses globally. Our results also merit consideration in the context of climate models used to estimate climate change impacts, but we caution against extrapolating the fertilization effect far into the future, which requires further assumptions on the functional form and the extent there are decreasing returns to further CO_2 increases as well as uncertainty about future environmental interactions.

While we reiterate that climate change will likely have a large negative impact on agriculture in aggregate, especially in regions exposed to extreme heat, and that CO_2-driven yield increases may be offset by effects on food nutrition and quality (Loladze 2002, Taub and Allen 2008, Myers et al. 2014), this paper demonstrates that marginal increases in CO_2 can also have strong countervailing fertilization effects—and that such effects may account for a material proportion of historical productivity improvements in US agriculture with

implications for the literature on agricultural productivity and structural transformation of economies.

References

Ainsworth, Elizabeth A., and Stephen P. Long. 2021. "30 years of free-air carbon dioxide enrichment (FACE): What have we learned about future crop productivity and its potential for adaptation?" *Global Change Biology* 27 (1): 27–49.

Ainsworth, Elizabeth A., and Alistair Rogers. 2007. "The response of photosynthesis and stomatal conductance to rising CO_2: mechanisms and environmental interactions." *Plant, Cell & Environment* 30 (3): 258–270.

Allen Jr., L. Hartwell, Jeff T. Baker, and Ken J. Boote. 1996. "The CO_2 fertilization effect: higher carbohydrate production and retention as biomass and seed yield."

Baker, Neil R. 2008. "Chlorophyll fluorescence: a probe of photosynthesis in vivo." *Annual Review of Plant Biology* 59 89–113.

Batts, G.R., J.I.L. Morison, R.H. Ellis, P. Hadley, and T.R. Wheeler. 1997. "Effects of CO_2 and temperature on growth and yield of crops of winter wheat over four seasons." *European Journal of Agronomy* 7 (1-3): 43–52.

Boone, Christopher, Wolfram Schlenker, and Juha Siikamäki. 2019. "Ground-Level Ozone and Corn Yields in the United States." *CEEP Working Paper 7*.

Bunce, J.A. 2012. "Responses of cotton and wheat photosynthesis and growth to cyclic variation in carbon dioxide concentration." *Photosynthetica* 50 (3): 395–400.

Crisp, David. 2015. "Measuring atmospheric carbon dioxide from space with the Orbiting Carbon Observatory-2 (OCO-2)." In *Earth Observing Systems XX*, Volume 9607. 960702. https://doi.org/10.1117/12.2187291.

Dell, Melissa, Benjamin F. Jones, and Benjamin A. Olken. 2014. "What Do We Learn from the Weather? The New Climate-Economy Literature." *Journal of Economic Literature* 53 (3): 740–798.

Didan, Kamel. 2015. "MOD13Q1 MODIS/Terra vegetation indices 16-day L3 global 250m SIN grid V006." *NASA EOSDIS Land Processes DAAC* 10.

Druckenmiller, Hannah, and Solomon Hsiang. 2019. "Accounting for Unobservable Heterogeneity in Cross Section Using Spatial First Differences." *NBER Working Paper 25177*.

Fitzgerald, Glenn J., Michael Tausz, Garry O'Leary et al. 2016. "Elevated atmospheric CO_2 can dramatically increase wheat yields in semi-arid environments and buffer against heat waves." *Global Change Biology* 22 (6): 2269–2284.

Gollin, Douglas, Casper Worm Hansen, and Asger Mose Wingender. 2021. "Two Blades of Grass: The Impact of the Green Revolution." *Journal of Political Economy* 129 (8): 2344–2384. https://doi.org/10.1086/714444.

Guan, Kaiyu, Joseph A. Berry, Yongguang Zhang, Joanna Joiner, Luis Guanter, Grayson Badgley, and David B. Lobell. 2016. "Improving the monitoring of crop productivity using spaceborne solar-induced fluorescence." *Global Change Biology* 22 (2): 716–726.

Hakkarainen, Janne, Iolanda Ialongo, and Johanna Tamminen. 2016. "Direct space-based observations of anthropogenic CO2 emission areas from OCO-2." *Geophysical Research Letters* 43 (21): 11–400.

Hungate, Bruce A., Jeffrey S. Dukes, M. Rebecca Shaw, Yiqi Luo, and Christopher B. Field. 2003. "Nitrogen and climate change." *Science* 302 (5650): 1512–1513.

Jacobson, Andrew R., Kenneth N. Schuldt, John B. Miller et al. 2020. "Carbon-Tracker CT2019B." https://doi.org/10.25925/20201008.

Jorgenson, Dale W., and Frank M. Gollop. 1992. "Productivity Growth in U.S. Agriculture: A Postwar Perspective." *American Journal of Agricultural Economics* 74 (3): 745–750, `http://www.jstor.org/stable/1242588`.

Keenan, Trevor F., David Y. Hollinger, Gil Bohrer, Danilo Dragoni, J. William Munger, Hans Peter Schmid, and Andrew D. Richardson. 2013. "Increase in forest water-use efficiency as atmospheric carbon dioxide concentrations rise." *Nature* 499 (7458): 324–327.

Kimball, B. A., C. F. Morris, P. J. Pinter Jr et al. 2001. "Elevated CO_2, drought and soil nitrogen effects on wheat grain quality." *New Phytologist* 150 (2): 295–303.

Kimball, Bruce A. 1983. "Carbon Dioxide and Agricultural Yield: An Assemblage and Analysis of 430 Prior Observations." *Agronomy Journal* 75 (5): 779–788.

Kimball, Bruce A. 2016. "Crop responses to elevated CO_2 and interactions with H_2O, N, and temperature." *Current Opinion in Plant Biology* 31 36–43.

Lambers, Hans, and Rafael S. Oliveira. 2019. "Photosynthesis, Respiration, and Long-Distance Transport: Photosynthesis." In *Plant Physiological Ecology*, 11–114, Springer.

Leakey, Andrew D.B., Martin Uribelarrea, Elizabeth A. Ainsworth, Shawna L. Naidu, Alistair Rogers, Donald R. Ort, and Stephen P. Long. 2006. "Photosynthesis, Productivity, and Yield of Maize Are Not Affected by Open-Air Elevation of CO_2 Concentration in the Absence of Drought." *Plant Physiology* 140 (2): 779–790.

Lobell, David B., and Senthold Asseng. 2017. "Comparing estimates of climate change impacts from process-based and statistical crop models." *Environmental Research Letters* 12 (1): 015001.

Loladze, Irakli. 2002. "Rising atmospheric CO_2 and human nutrition: toward globally imbalanced plant stoichiometry?" *Trends in Ecology & Evolution* 17 (10): 457–461.

Long, Stephen P., Elizabeth A. Ainsworth, Andrew D. B. Leakey, Josef Nösberger, and Donald R. Ort. 2006. "Food for Thought: Lower-Than-Expected Crop Yield Stimulation with Rising CO_2 Concentrations." *Science* 312 (5782): 1918–1921.

Long, Stephen P., Elizabeth A. Ainsworth, Alistair Rogers, and Donald R. Ort. 2004. "Rising atmospheric carbon dioxide: plants FACE the future." *Annual Review of Plant Biology* 55 591–628.

Markelz, R. J. Cody, Reid S. Strellner, and Andrew D. B. Leakey. 2011. "Impairment of C_4 photosynthesis by drought is exacerbated by limiting nitrogen and ameliorated by elevated CO_2 in maize." *Journal of Experimental Botany* 62 (9): 3235–3246.

McGrath, Justin M., and David B. Lobell. 2013. "Regional disparities in the CO_2 fertilization effect and implications for crop yields." *Environmental Research Letters* 8 (1): 014054.

Moore, Frances C., Uris Lantz C. Baldos, and Thomas Hertel. 2017. "Economic impacts of climate change on agriculture: a comparison of process-based and statistical yield models." *Environmental Research Letters* 12 (6): 065008.

Morgan, Jack A., Daniel R. LeCain, Elise Pendall et al. 2011. "C4 grasses prosper as carbon dioxide eliminates desiccation in warmed semi-arid grassland." *Nature* 476 (7359): 202–205.

Mortensen, Leiv M. 1987. "CO_2 Enrichment in Greenhouses. Crop Responses." *Scientia Horticulturae* 33 (1-2): 1–25.

Myers, Samuel S., Antonella Zanobetti, Itai Kloog et al. 2014. "Increasing CO_2 threatens human nutrition." *Nature* 510 (7503): 139–142.

Ottman, M. J., B. A. Kimball, P.J. Pinter et al. 2001. "Elevated CO_2 increases sorghum biomass under drought conditions." *New Phytologist* 150 (2): 261–273.

Reich, Peter B., Sarah E. Hobbie, Tali Lee et al. 2006. "Nitrogen limitation constrains sustainability of ecosystem response to CO_2." *Nature* 440 (7086): 922–925.

Sanders, Nicholas J, and Alan Barreca. 2021. "Adaptation to Environmental Change: Agriculture and the Unexpected Incidence of the Acid Rain Program."Technical report, National Bureau of Economic Research.

Schlenker, Wolfram, and Michael J. Roberts. 2009. "Nonlinear Temperature Effects Indicate Severe Damages to U.S. Crop Yields under Climate Change." *Proceedings of the National Academy of Sciences* 106 (37): 15594–15598.

Sun, Ying, Christian Frankenberg, Martin Jung, Joanna Joiner, Luis Guanter, Philipp Köhler, and Troy Magney. 2018. "Overview of Solar-Induced chlorophyll Fluorescence (SIF) from the Orbiting Carbon Observatory-2: Retrieval, cross-mission comparison, and global monitoring for GPP." *Remote Sensing of Environment* 209 808–823.

Tack, Jesse, Andrew Barkley, and Lawton Lanier Nalley. 2015. "Effect of Warming temperatures on US Wheat Yields." *Proceedings of the National Academy of Sciences* 112 (22): 6931–6936.

Taub, Daniel R., and Brian Millerand Holly Allen. 2008. "Effects of elevated CO_2 on the protein concentration of food crops: a meta-analysis." *Global Change Biology* 14 (3): 565–575.

Toreti, Andrea, Delphine Deryng, Francesco N. Tubiello et al. 2020. "Narrowing uncertainties in the effects of elevated CO_2 on crops." *Nature Food* 1 (12): 775–782.

Tubiello, Francesco N., Jeffrey S. Amthor, Kenneth J.Boote et al. 2007. "Crop response to elevated CO2 and world food supply: A comment on "Food for Thought ..." by Long et al., Science 312:1918–1921, 2006." *European journal of agronomy* 26 (3): 215–223.

Wang, Songhan, Yongguang Zhang, Weimin Ju et al. 2020. "Recent global decline of CO_2 fertilization effects on vegetation photosynthesis." *Science* 370 (6522): 1295–1300.

Wang, Sun Ling, Paul Heisey, David Schimmelpfennig, and V. Eldon Ball. 2015. "Agricultural Productivity Growth in the United States: Measurement, Trends, and Drivers." *Economic Research Service, Paper No. 189.*

Yin, Yi, Brendan Byrne, Junjie Liu et al. 2020. "Cropland carbon uptake delayed and reduced by 2019 Midwest floods." *AGU Advances* 1 (1): e2019AV000140. https://doi.org/10.1029/2019AV000140.

Zheng, Yunpu, Chunlin He, Lili Guo, Lihua Hao, Dongjuan Cheng, Fei Li, Zhengping Peng, and Ming Xu. 2020. "Soil water status triggers CO_2 fertilization effect on the growth of winter wheat (Triticum aestivum)." *Agricultural and Forest Meteorology* 291 108097.

Zhu, Zaichun, Shilong Piao, Ranga B. Myneni et al. 2016. "Greening of the Earth and its Drivers." *Nature climate change* 6 (8): 791–795.

Ziska, Lewis H., and James A. Bunce. 2007. "Predicting the impact of changing CO_2 on crop yields: some thoughts on food." *New Phytologist* 175 (4): 607–618.

Figure 1: Annual Yields and CO_2

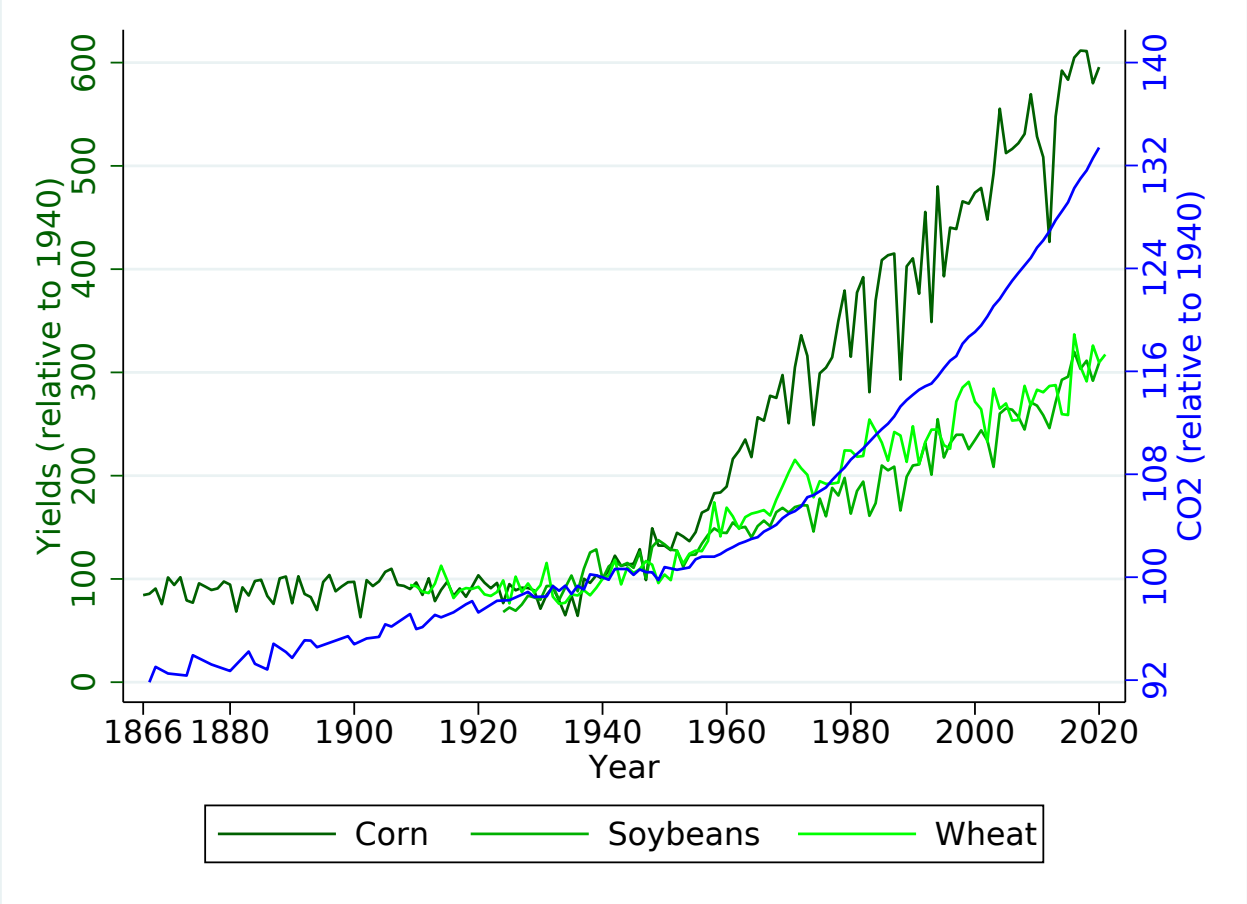

Notes: Figure displays the evolution of yearly aggregate US yields (left axis) and annual CO_2 averages (right axis). Each time series is normalized relative to 1940 (value = 100). Aggregate US corn yields are shown in dark green from 1866-2020, aggregate US soybeans yields in green from 1924-2020, and aggregate US winter wheat yields in light green from 1909-2020, the years for which the data is reported by the National Agricultural Statistics Service (NASS) by USDA. The annual average CO_2 estimate is added in blue from NOAA.

Figure 2: Identifying Variation Used in Analysis

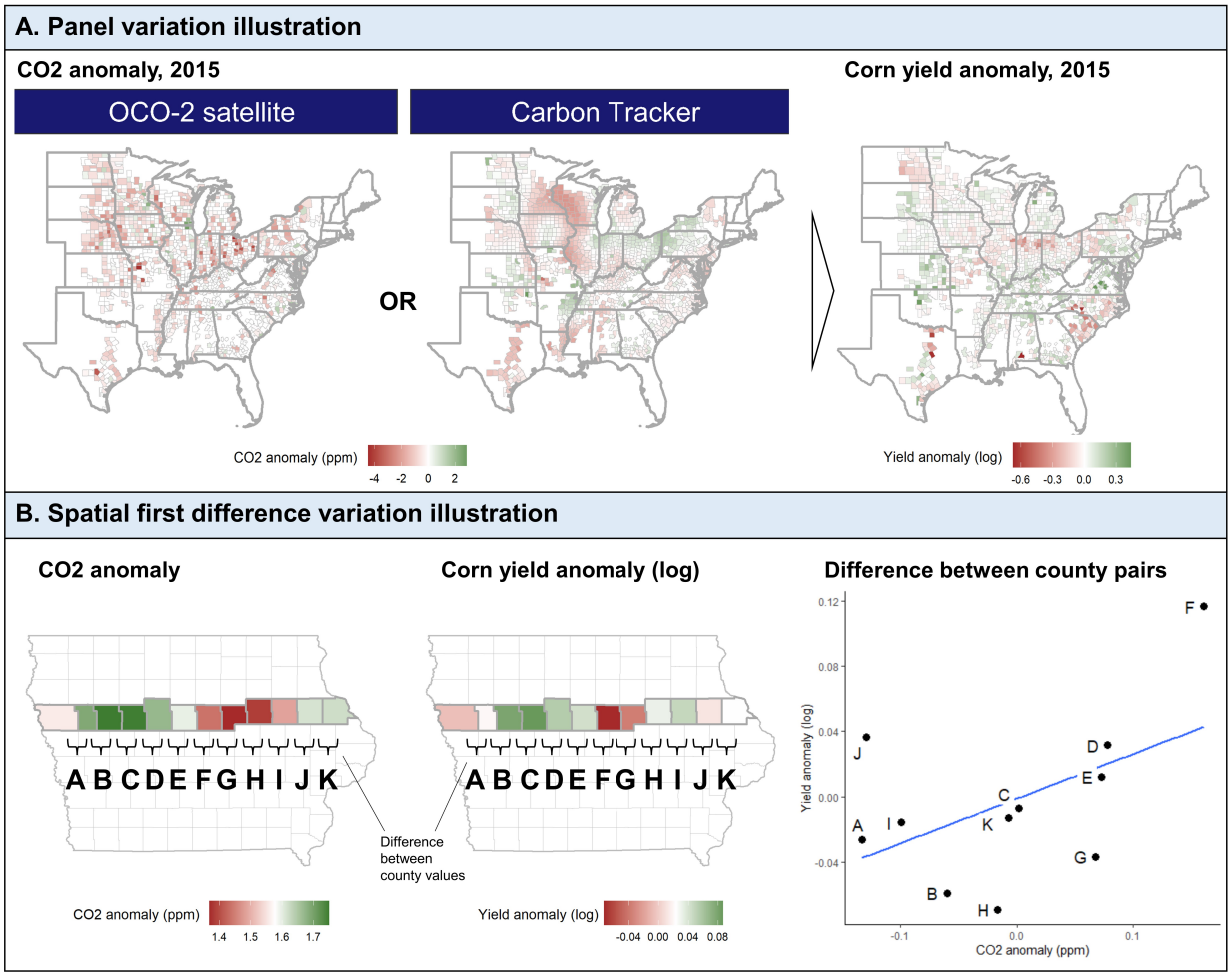

Notes: Top panel (A) illustrates the empirical variation used in the panel models, in which CO_2 anomalies as measured by OCO-2 and CarbonTracker (top left and middle charts) relate to yield anomalies (top right chart) in example year 2015. Anomalies are obtained after accounting for county fixed effects (averages) and county-specific time trends. Note that our actual panel regressions include additional years beyond 2015 and all counties east of the Rockies. Bottom panel (B) illustrates the variation used in the spatial first difference (SFD) models. For counties spanning an example latitude band in Iowa, each letter (A to K) represents the difference in CO_2 and yield anomalies between neighboring counties (bottom left and middle charts) in example year 2016. The bottom right chart plots these differences to showcase the relationship. Note that in our actual SFD regressions we include as observations all neighboring gradients and not just horizontal ones, as well as all counties in the US.

Figure 3: CO_2 Fertilization Effects

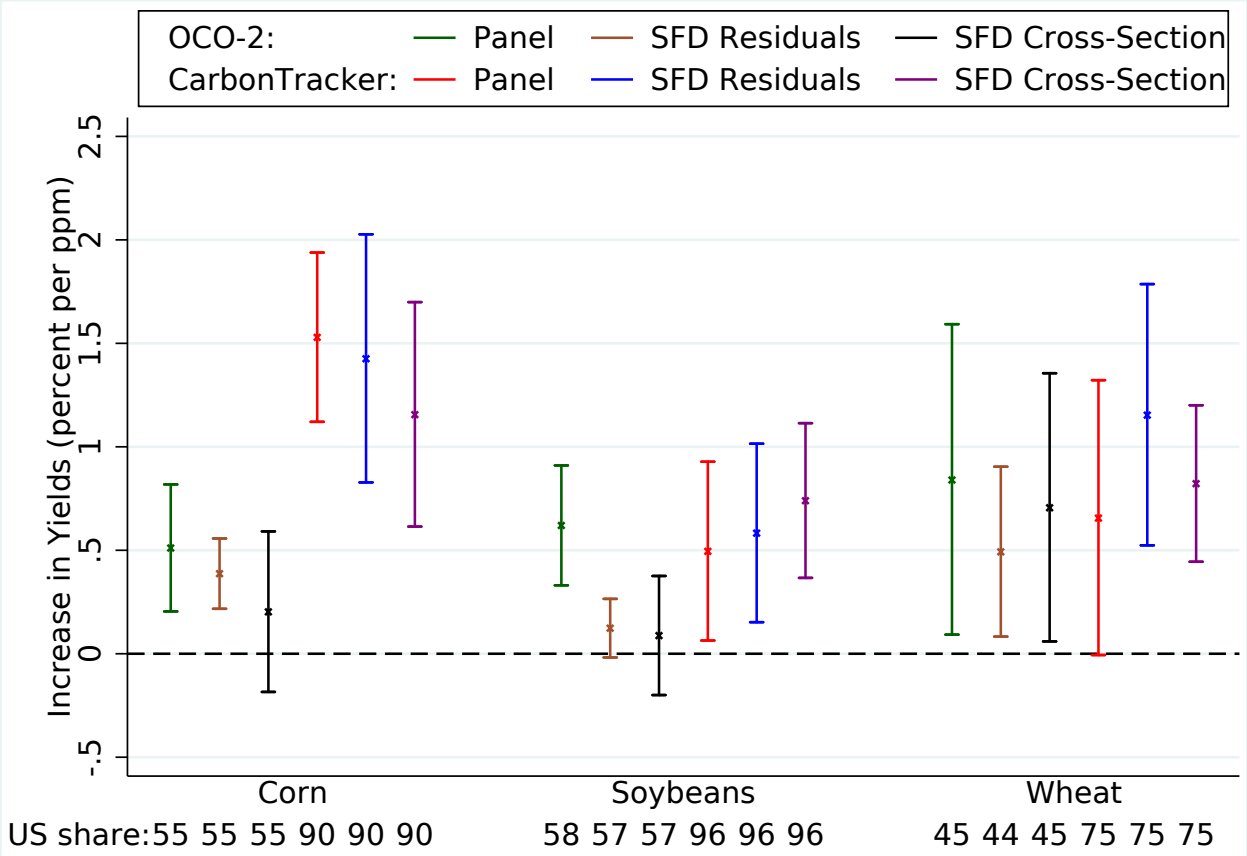

Notes: Figure displays the CO_2 fertilization effect of an increase in CO_2 concentration by 1 ppm on aggregate yields in the sample for corn, soybeans and wheat. The point estimates are marked by an x, and the 90% confidence intervals are added as lines. Figure displays three sources of variation. The panel results regress the log of county-level yields on seasonality-adjusted CO_2, weather variables (Schlenker and Roberts 2009), controls for other pollutants (CO, NO_2, O_3, PM_{10}, SO_2), county fixed effects and county-specific time trends. The spatial first difference (SFD Residuals) looks at the change in the anomalies between neighboring counties in a given year after removing county fixed effects and county-specific time trends. It links changes in the log yield anomalies to changes in CO_2 anomalies as well as anomalies of the weather and pollution variables. The spatial first difference (SFD Cross-section) looks at changes in the average outcome for each variable between neighbors, linking again changes in the average of log yield to average CO_2 as well as average weather and pollution. The first three estimates for each crop use satellite readings from OCO-2 (2015-2020), while the last three use data from CarbonTracker (2000-2018). The bottom row displays the share of US production in the estimation sample for those years.

Appendix:
Environmental Drivers of Agricultural Productivity Growth: CO_2 Fertilization of US Field Crops

Charles A. Taylor[1] and Wolfram Schlenker[1,2]

List of Figures

List of Tables

[1] School of International and Public Affairs, Columbia University, 420 West 118th St., New York, NY 10027.
[2] National Bureau of Economic Research (NBER), 1050 Massachusetts Ave., Cambridge, MA 02138.

Figure A1: Seasonality in CO_2 and SIF

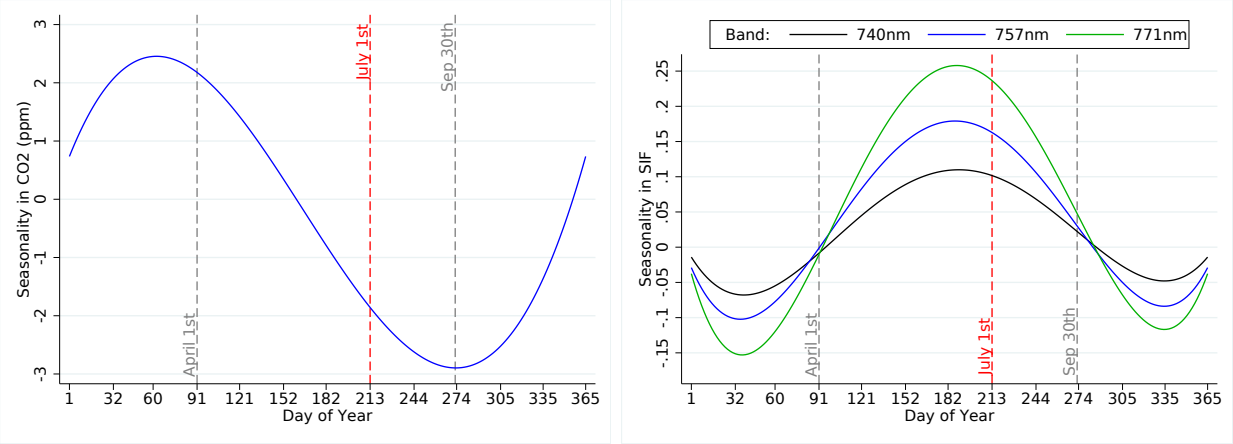

Notes: Left chart displays the seasonality in CO_2, the right chart shows the seasonality of solar-induced chlorophyll fluorescence (SIF) for the 740nm, 757nm and 771nm bands. To make readings comparable, they are seasonality-adjusted to July 1st (red dashed line) of that year, i.e., a reading on a particular day is corrected by the difference between the July 1st value of the above seasonality curve and the value of the seasonality curve on the day of the measurement. The seasonality curves are estimated using all OCO2 readings without quality fags over the contiguous US using a 4^{th}-order Chebyschev polynomial in the day of year as well as a linear time trend. Since years have different numbers of days, we normalize January 1st to -1 and December 31st to 1. The seasonality regression is constraint so the value at the end of the year (December 31st) equals the value at the beginning of the year (January 1st). The main growing season for corn and soybeans (April-September) is added as grey dashed lines.

Figure A2: Number of Observations per County - Corn

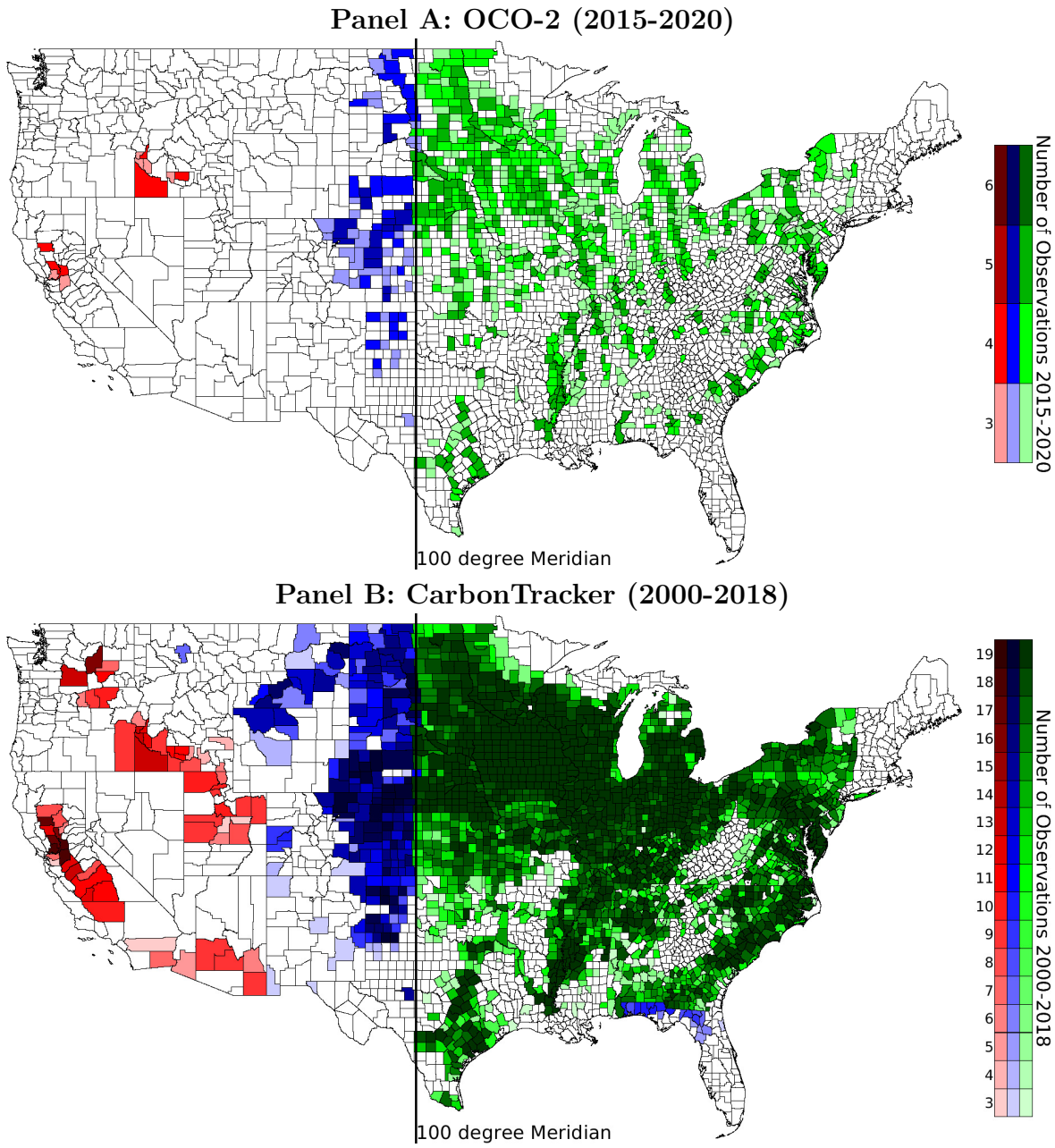

Notes: Figure displays the number of observations per county in the date set, i.e., where both yield data and CO_2 data are available. The top panel shows the number of observations for the six years 2015-2020 where OCO-2 data are available. The bottom panel shows the number of observations in 2000-2018 where CarbonTracker data are available. We split the analysis into three geographic subsets: east of the 100° meridian excluding Florida (Schlenker and Roberts 2009) shown in shades of green, arid Western United States (California, Arizona, Utah, Nevada, Oregon, Idaho, and Washington) shown in red, and the remaining counties shown in blue. Since our specification includes county fixed effects and county-specific time trends, we require at least 3 observation to be included in the dataset.

Figure A3: Number of Observations per County - Soybeans

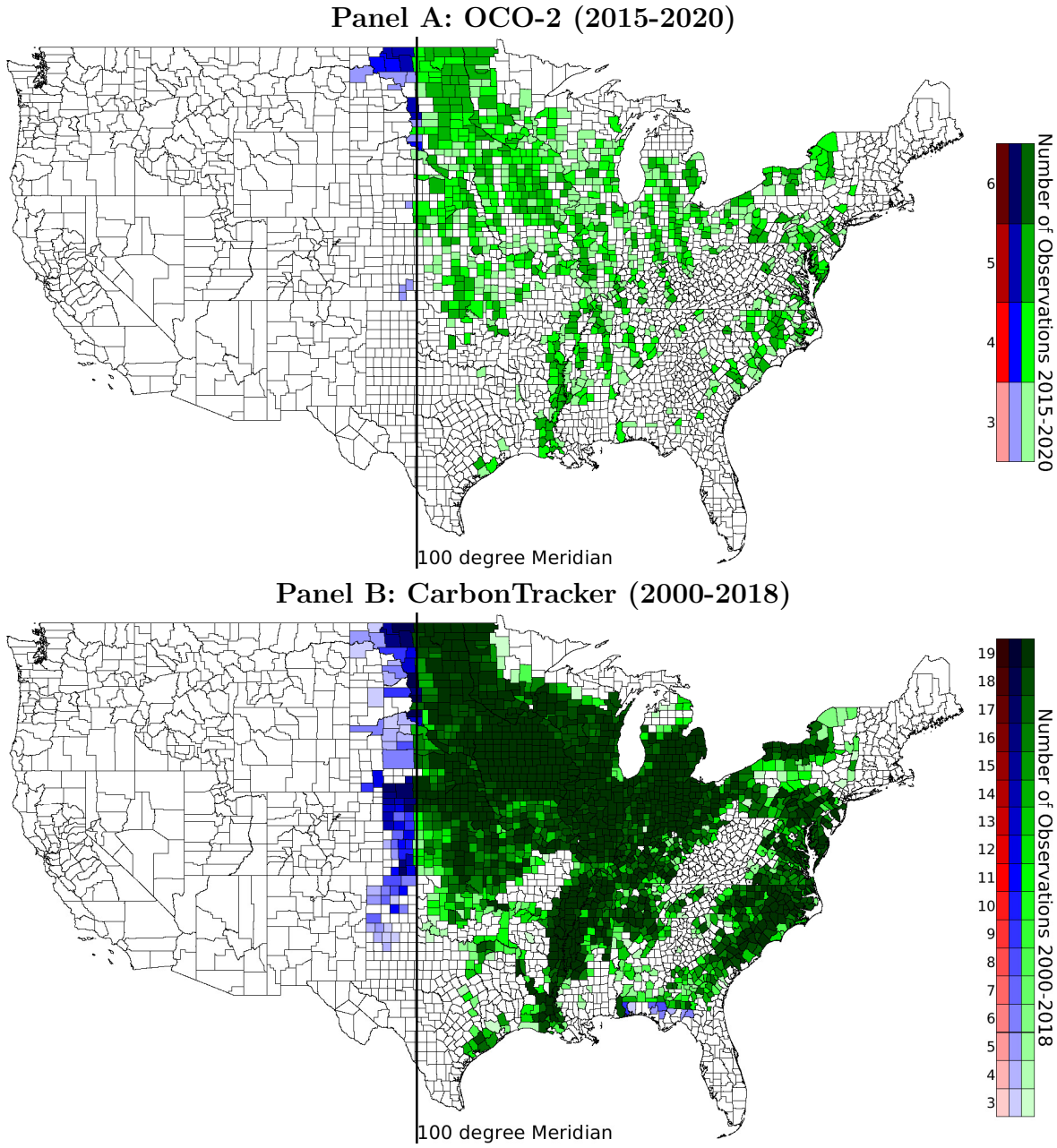

Notes: Figure displays the number of observations per county in the date set, i.e., where both yield data and CO_2 data are available. The top panel shows the number of observations for the six years 2015-2020 where OCO-2 data are available. The bottom panel shows the number of observations in 2000-2018 where CarbonTracker data are available. We split the analysis into three geographic subsets: east of the 100° meridian excluding Florida (Schlenker and Roberts 2009) shown in shades of green, arid Western United States (California, Arizona, Utah, Nevada, Oregon, Idaho, and Washington) shown in red, and the remaining counties shown in blue. Since our specification includes county fixed effects and county-specific time trends, we require at least 3 observation to be included in the dataset.

Figure A4: Number of Observations per County - Winter Wheat

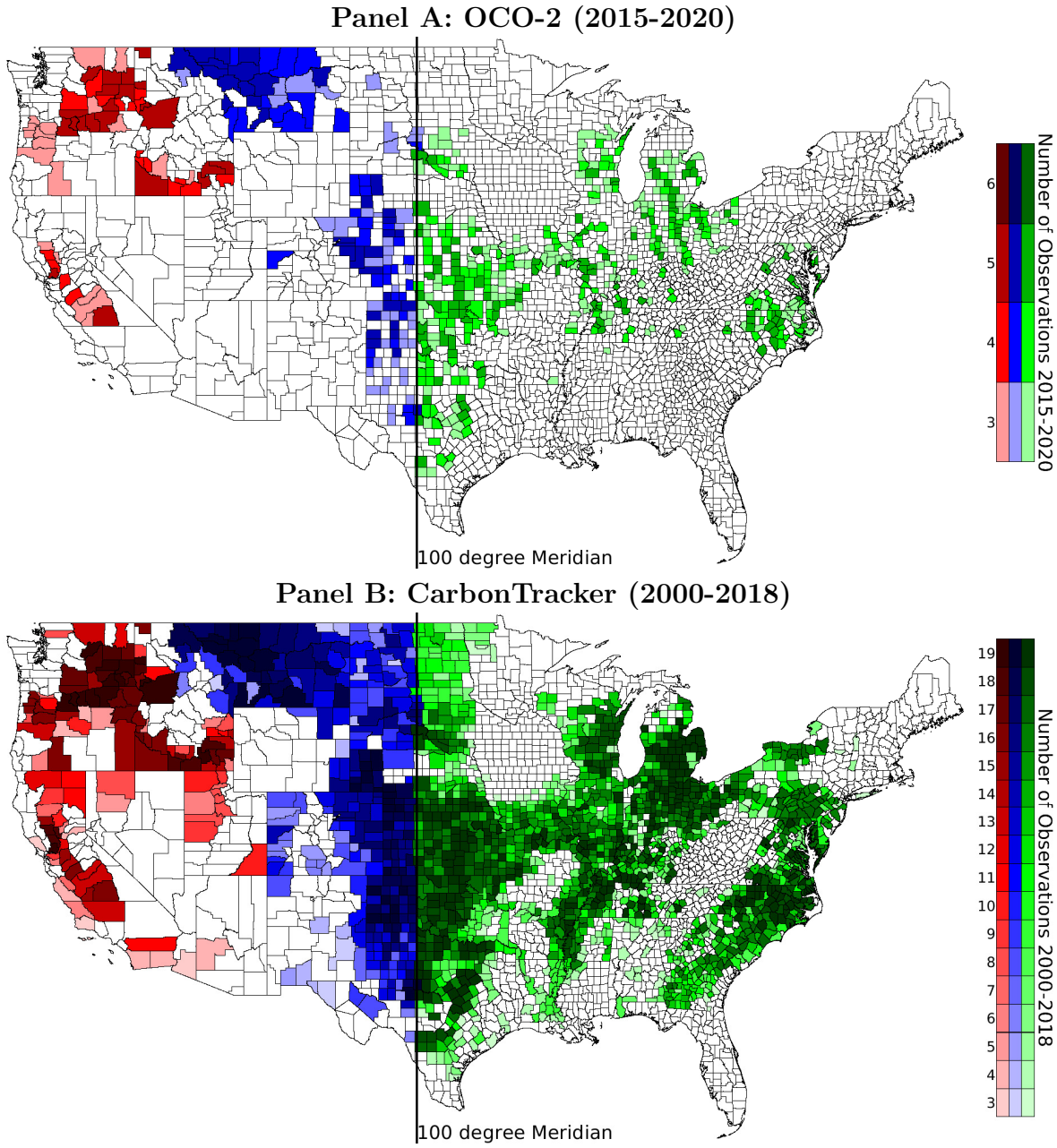

Notes: Figure displays the number of observations per county in the date set, i.e., where both yield data and CO_2 data are available. The top panel shows the number of observations for the six years 2015-2020 where OCO-2 data are available. The bottom panel shows the number of observations in 2000-2018 where CarbonTracker data are available. We split the analysis into three geographic subsets: east of the 100° meridian excluding Florida (Schlenker and Roberts 2009) shown in shades of green, arid Western United States (California, Arizona, Utah, Nevada, Oregon, Idaho, and Washington) shown in red, and the remaining counties shown in blue. Since our specification includes county fixed effects and county-specific time trends, we require at least 3 observation to be included in the dataset.

Figure A5: Identifying Variation Used in Analysis

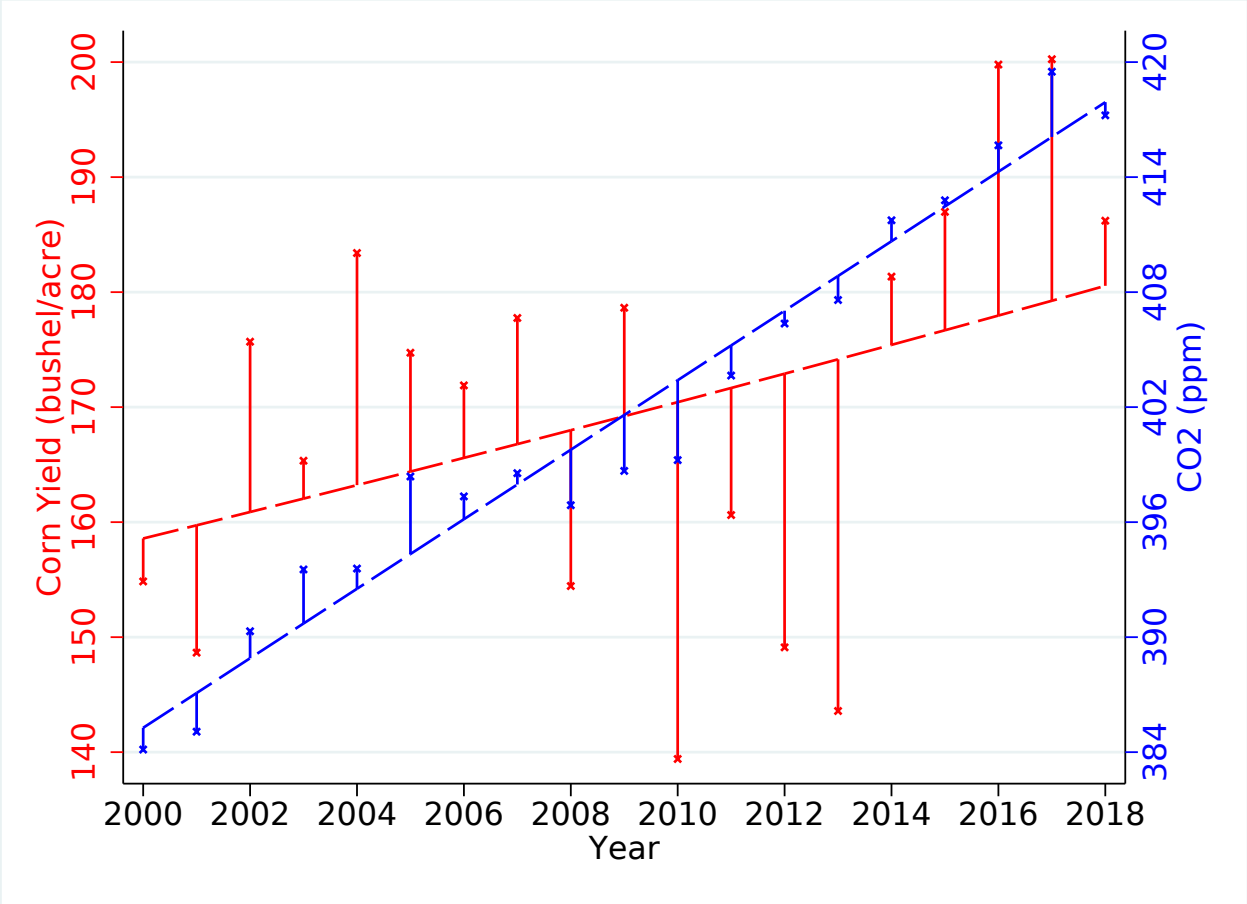

Notes: Figure displays the variation used in the statistical analysis. We include county-fixed effects and county-specific time trends. This is equivalent to fitting a time trend (shown as dashed lines) to both yields and CO_2 readings for each county and then looking at the residuals. The above figure shows this for the more urban Polk county in Iowa (FIPS code 19153), the county where Des Moines is located and CO_2 anomalies are less driven by agriculture itself. Corn anomalies are shown as solid red lines, while CO_2 anomalies are shown as blue lines. When CO_2 positively (negatively) deviates from the trend, so do yields. Figure A6 shows the cross-plot for all observations (counties and years) after additionally removing the effect of weather and other pollutants.

Figure A6: Scatter Plots of Log Yield Anomalies against CO_2 Anomalies

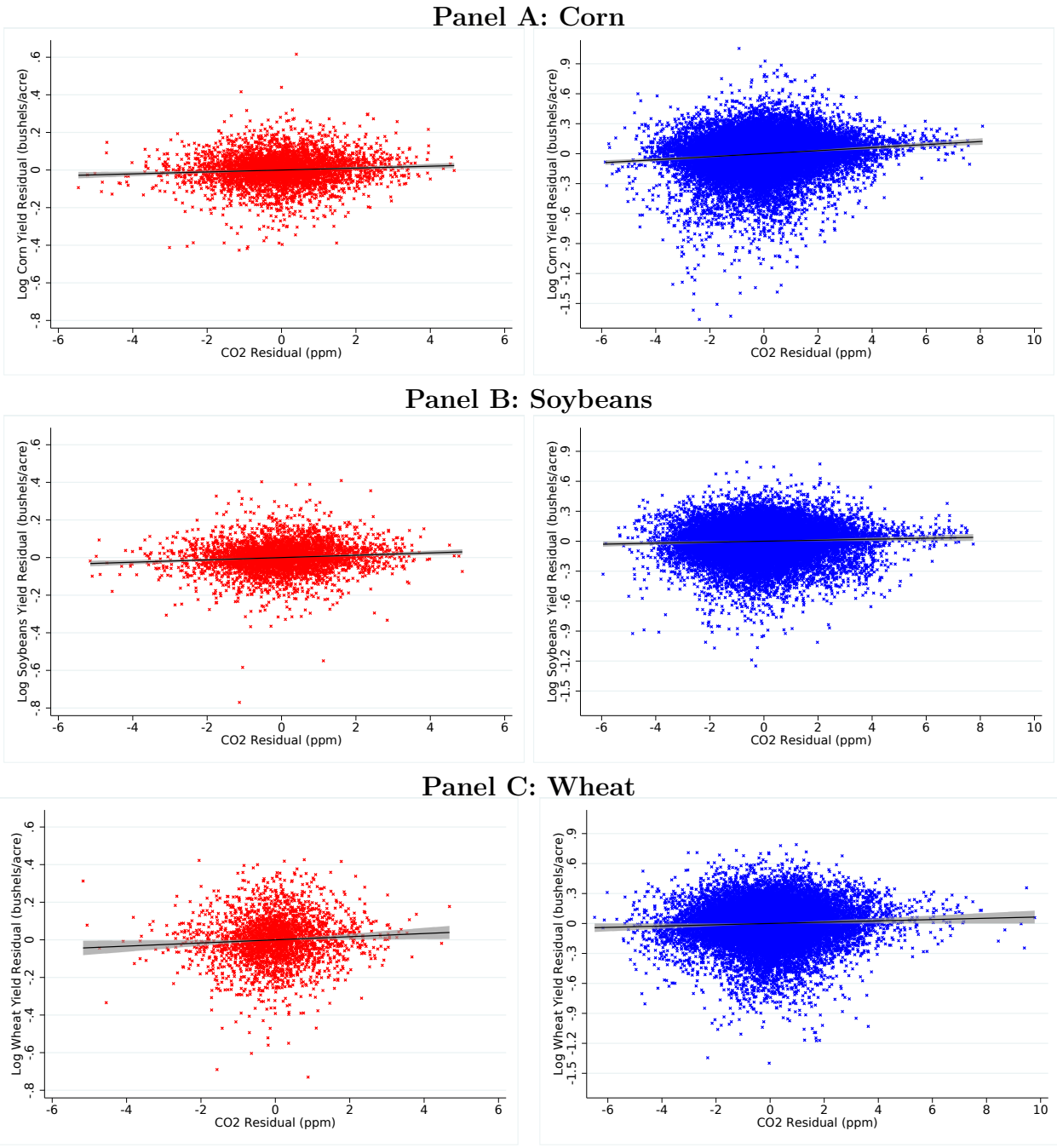

Notes: Figure summarizes anomalies after county fixed effects, county-specific time trends, the four weather variables, and five pollutants are partialled out. This is the variation we use to identify the effect of CO_2 on yields in the panel regressions in Figure 3. The top graphs displays the results for corn, the middle for soybeans, and the bottom for winter wheat. The left column uses OCO-2 satellite readings, the right column data from CarbonTracker. The regression results on the CO_2 fertilization effect are shown as solid line with 90% confidence interval added in grey. In the CarbonTracker data there is one outlier for soybeans and four for wheat that are not shown in the picture, but including or excluding them has no effect given the large sample size.

Figure A7: Crossplots of CO_2 Anomalies in CarbonTracker and OCO-2 (2015-2018)

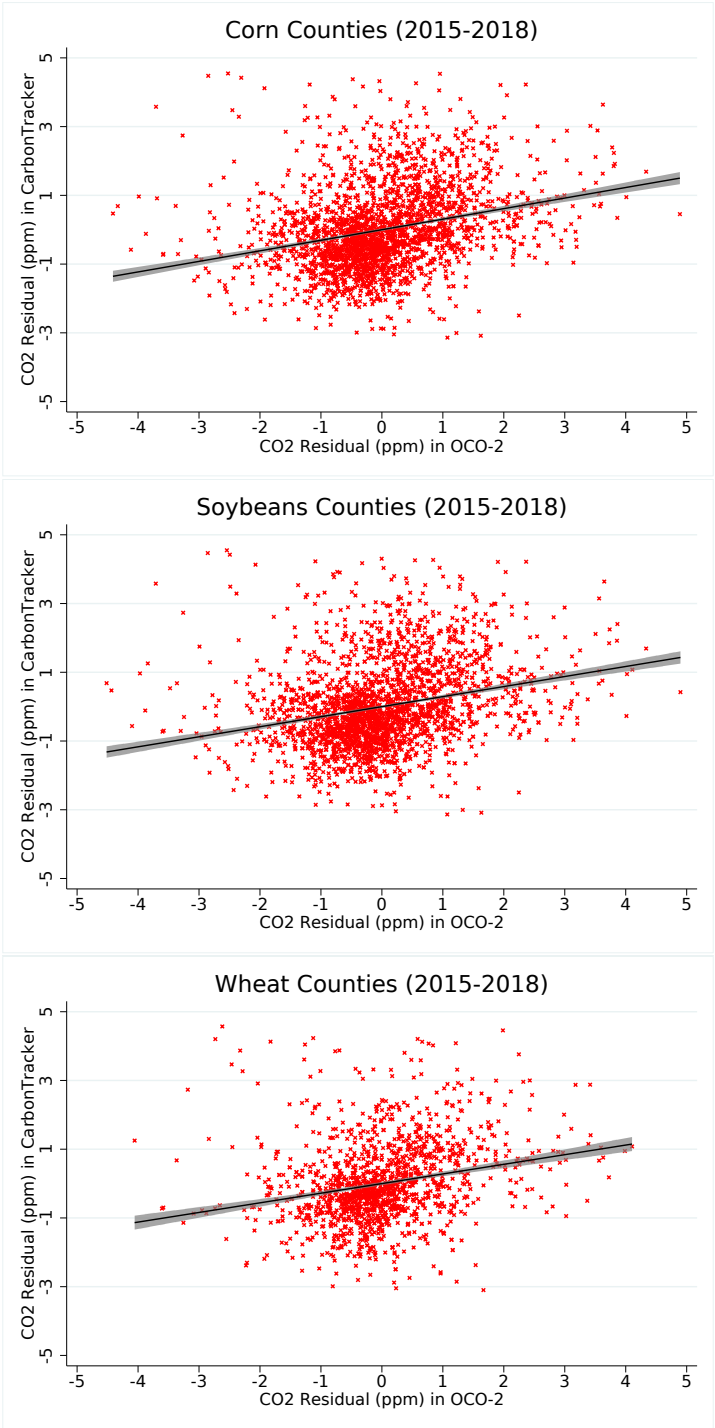

Notes: Figure displays the cross-plot of CO_2 anomalies in CarbonTracker and OCO-2 satellite readings. The two data sources only overlap for four years (2015-2018). We include county-year observations east of the Rocky Mountains that have at least three observations for both CO_2 measures so we can fit county fixed effects and county-specific time trends. The grey regression line shows the results of a first-stage regression that instruments the CarbonTracker data with OCO-2 readings.

Figure A8: Sensitivity Check: Log-Log Model Specification

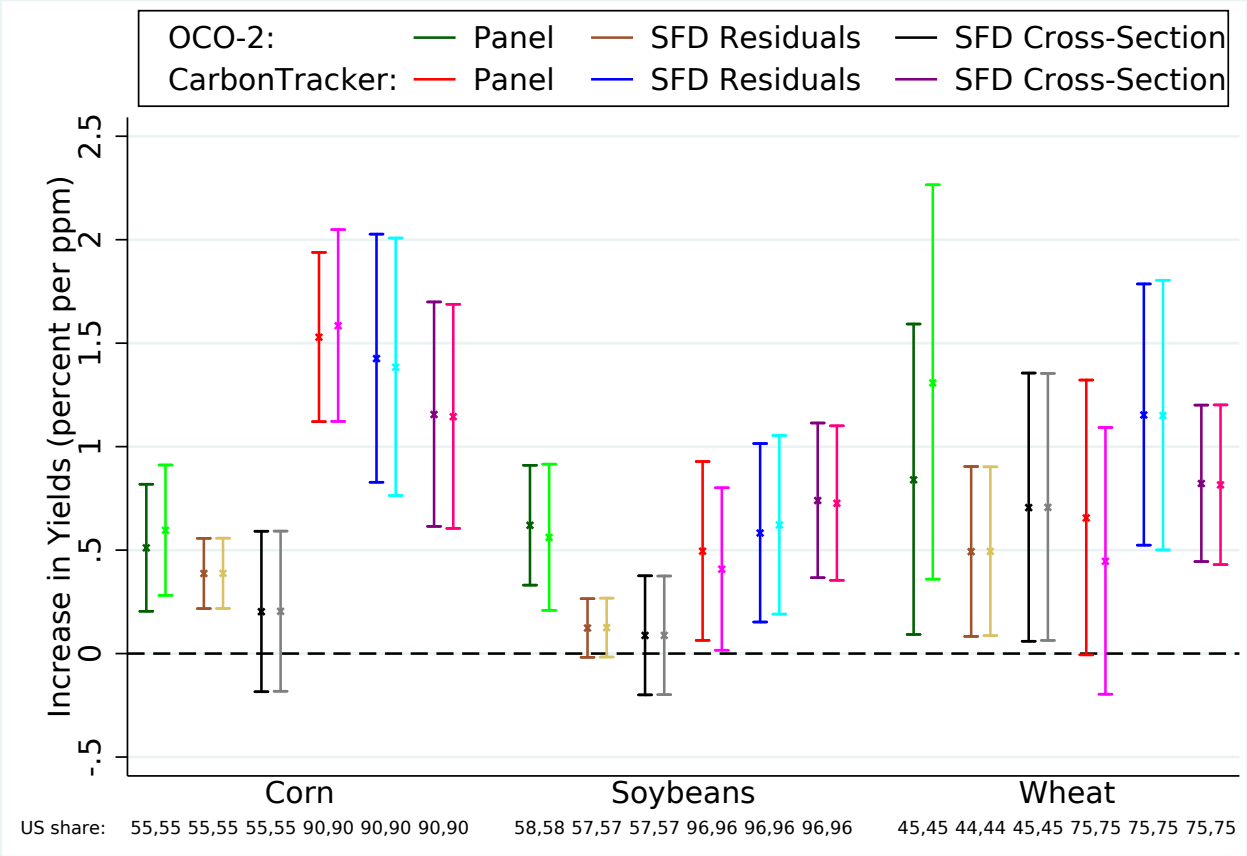

Notes: Figure replicates Figure 3 shown in darker colors for reference. The lighter colors rerun each specification (panel or spatial first difference (SFD) using both the OCO-2 and CarbonTracker dataset), expect that it uses the log of CO_2 rather than CO_2 levels as explanatory variable. Graphs display the CO_2 fertilization effect of an increase in CO_2 concentration by 1 ppm on aggregate yields in the sample for corn, soybeans and wheat. The point estimates are marked by an x, and the 90% confidence intervals are added as lines. The bottom rows display the share of US production in the estimation sample.

Figure A9: Sensitivity Check: Lin-Lin Model Specification

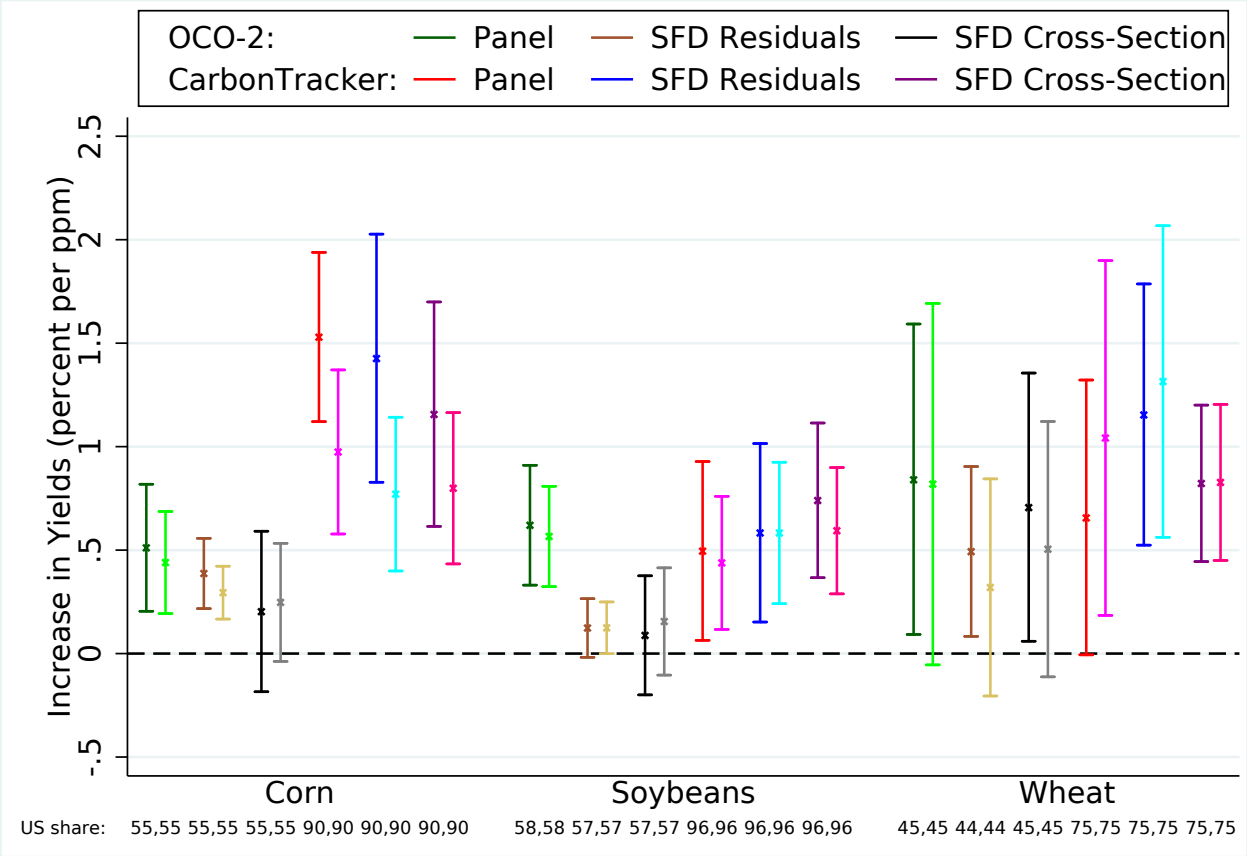

Notes: Figure replicates Figure 3 shown in darker colors for reference. The lighter colors rerun each specification (panel or spatial first difference (SFD) using both the OCO-2 and CarbonTracker dataset), expect that the dependent variable is yields instead of log yields. Graphs display the CO_2 fertilization effect of an increase in CO_2 concentration by 1 ppm on aggregate yields in the sample for corn, soybeans and wheat. The point estimates are marked by an x, and the 90% confidence intervals are added as lines. The bottom rows display the share of US production in the estimation sample.

Figure A10: Sensitivity Check: Lin-Log Model Specification

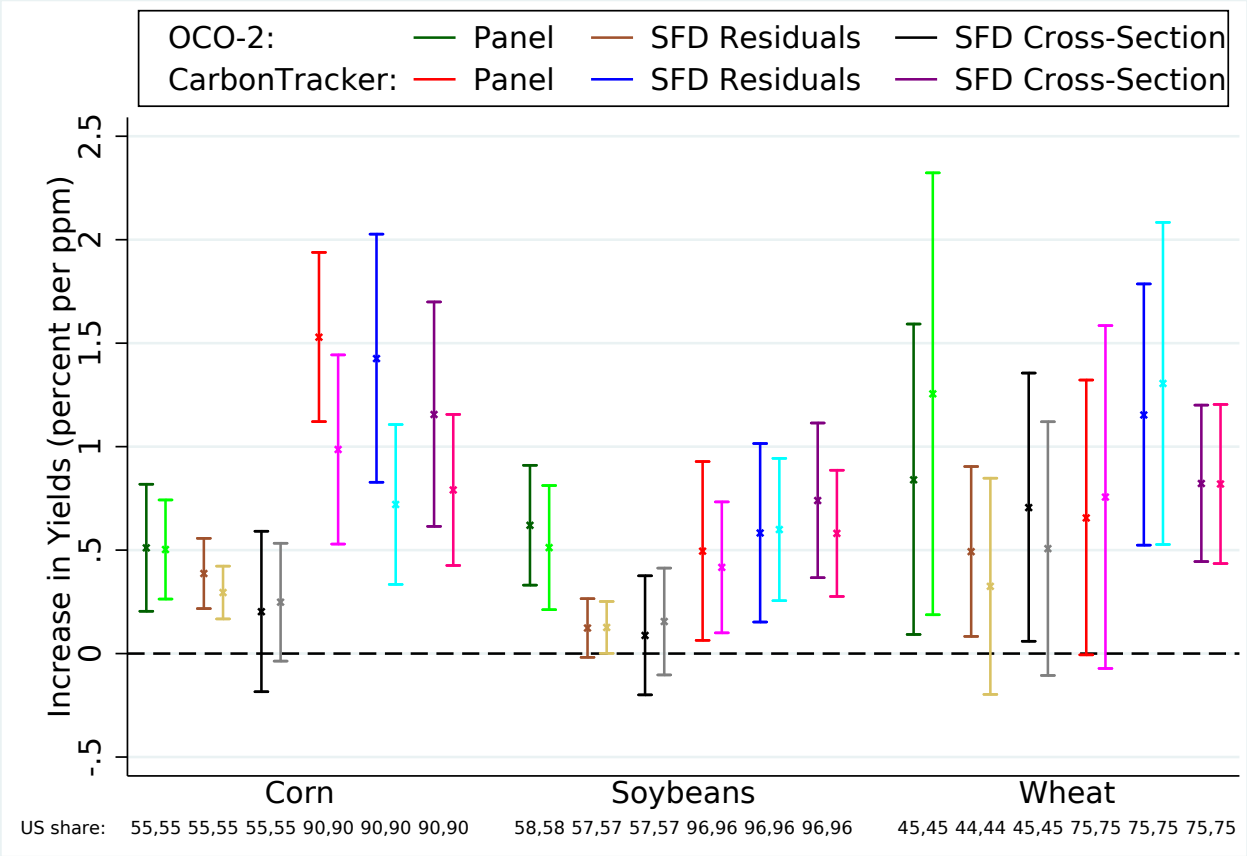

Notes: Figure replicates Figure 3 shown in darker colors for reference. The lighter colors rerun each specification (panel or spatial first difference (SFD) using both the OCO-2 and CarbonTracker dataset), expect that yields are linked to the log of CO_2 levels rather than linking log yields to CO_2 levels in the baseline. Graphs display the CO_2 fertilization effect of an increase in CO_2 concentration by 1 ppm on aggregate yields in the sample for corn, soybeans and wheat. The point estimates are marked by an x, and the 90% confidence intervals are added as lines. The bottom rows display the share of US production in the estimation sample.

Figure A11: Sensitivity Check: State-Specific Time Trends

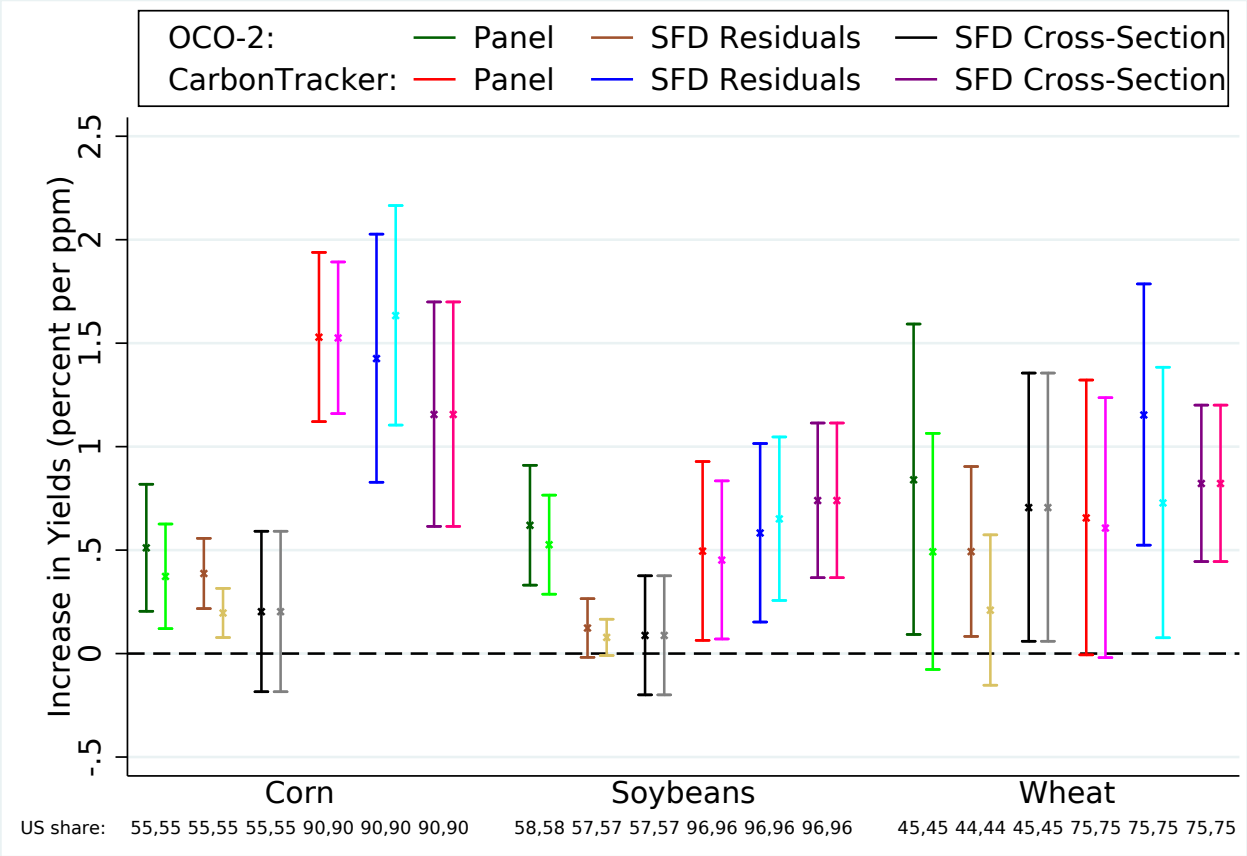

Notes: Figure replicates Figure 3 shown in darker colors for reference. The lighter colors rerun each specification (panel or spatial first difference (SFD) using both the OCO-2 and CarbonTracker dataset), using state-specific time trends to calculate the anomalies rather than county-specific time trends in the baseline. Graphs display the CO_2 fertilization effect of an increase in CO_2 concentration by 1 ppm on aggregate yields in the sample for corn, soybeans and wheat. The point estimates are marked by an x, and the 90% confidence intervals are added as lines. The bottom rows display the share of US production in the estimation sample.

Figure A12: Sensitivity Check: No Time Trend

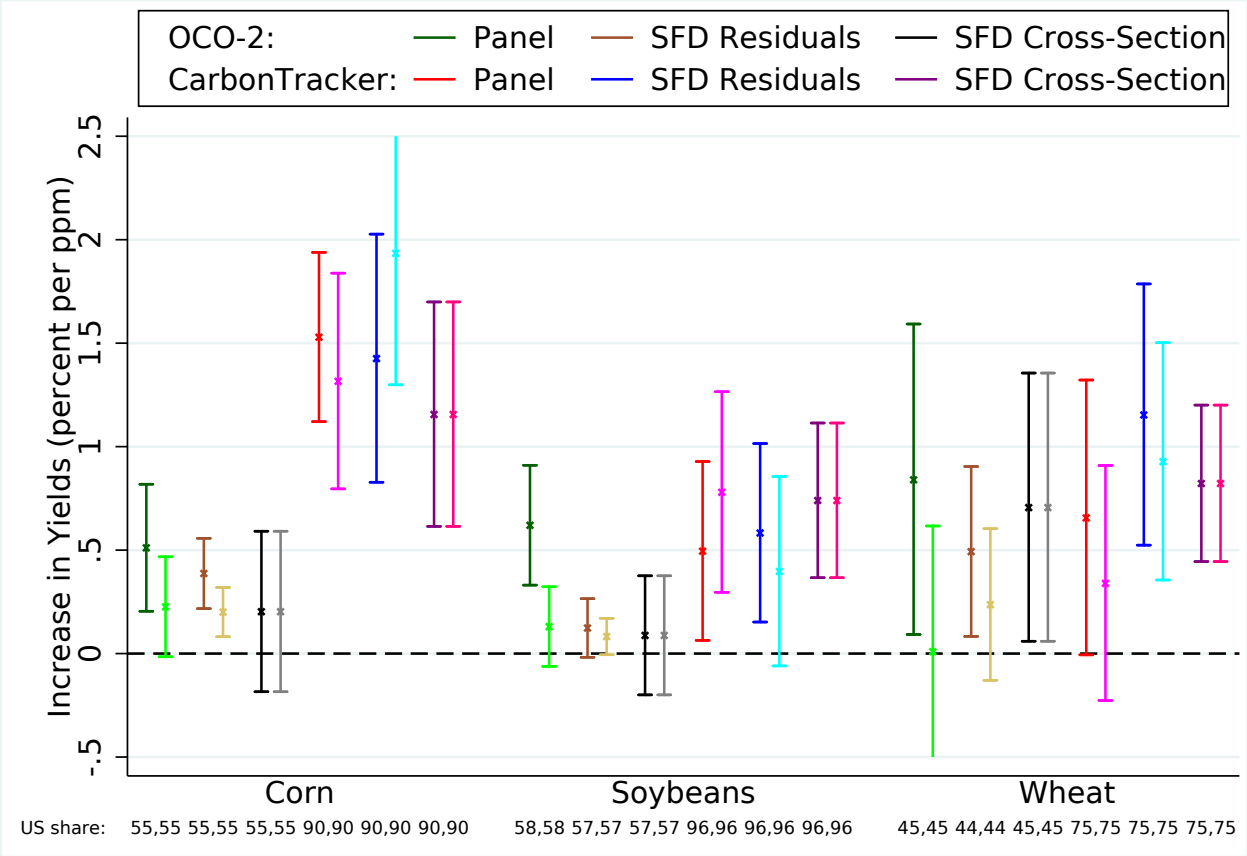

Notes: Figure replicates Figure 3 shown in darker colors for reference. The lighter colors rerun each specification (panel or spatial first difference (SFD) using both the OCO-2 and CarbonTracker dataset), using no time trends across the US to calculate the anomalies rather than county-specific time trends in the baseline. Graphs display the CO_2 fertilization effect of an increase in CO_2 concentration by 1 ppm on aggregate yields in the sample for corn, soybeans and wheat. The point estimates are marked by an x, and the 90% confidence intervals are added as lines. The bottom rows display the share of US production in the estimation sample.

Figure A13: Sensitivity Check: Data From Entire Contiguous US

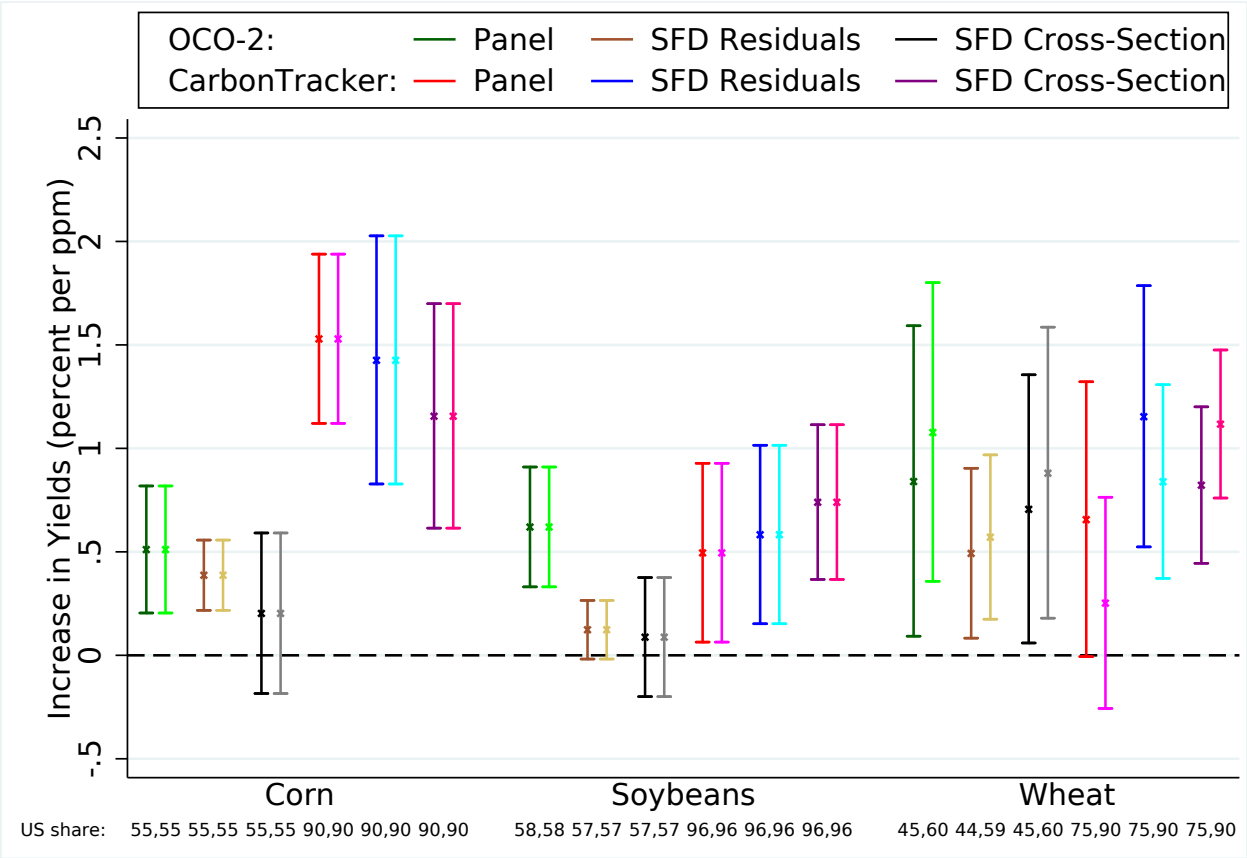

Notes: Figure replicates Figure 3 shown in darker colors for reference. The lighter colors rerun each specification (panel or spatial first difference (SFD) using both the OCO-2 and CarbonTracker dataset), using all counties in the contiguous US rather than just the ones east of the Rocky Mountains (colored green or blue in Figures A2-A4. Graphs display the CO_2 fertilization effect of an increase in CO_2 concentration by 1 ppm on aggregate yields in the sample for corn, soybeans and wheat. The point estimates are marked by an x, and the 90% confidence intervals are added as lines. The bottom rows display the share of US production in the estimation sample.

Figure A14: Sensitivity Check: Data From Counties East of 100° Meridian

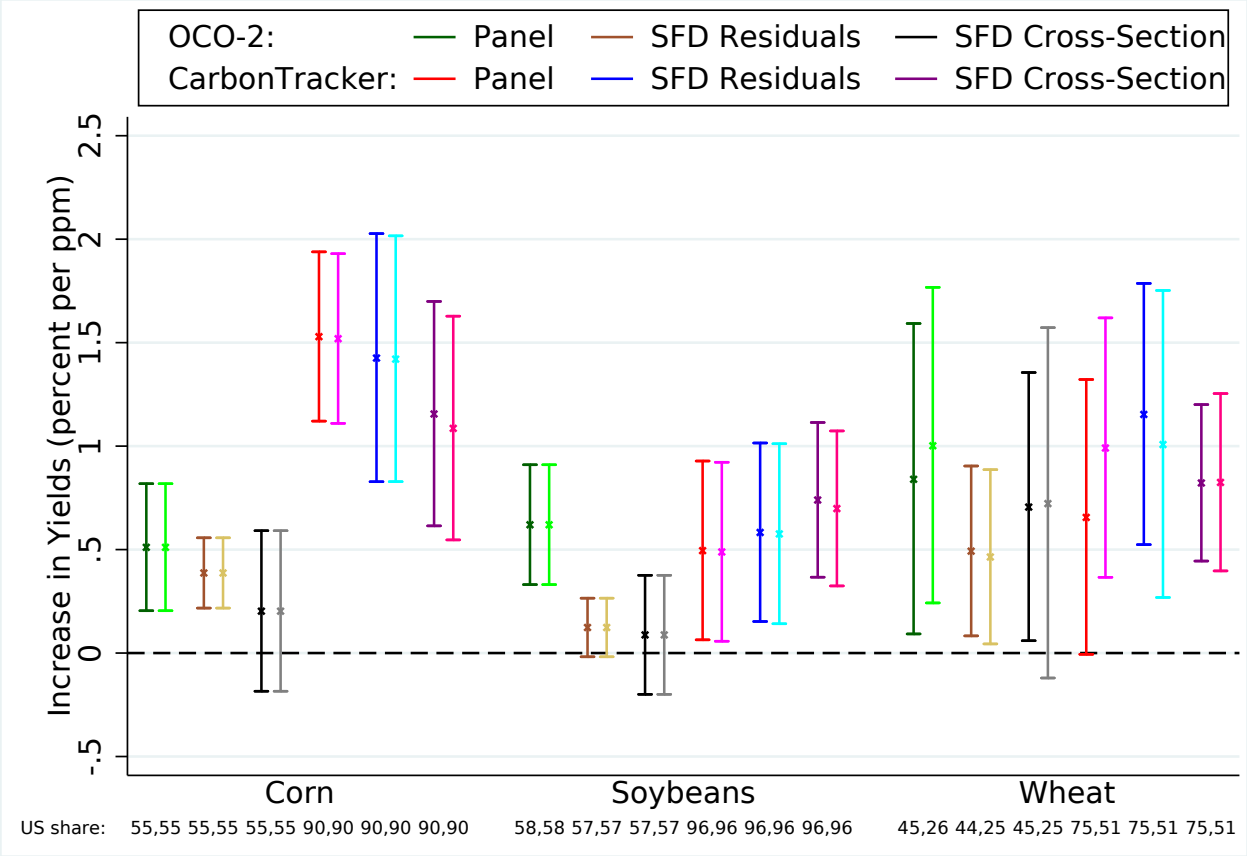

Notes: Figure replicates Figure 3 shown in darker colors for reference. The lighter colors rerun each specification (panel or spatial first difference (SFD) using both the OCO-2 and CarbonTracker dataset), using counties east of the 100° meridian except Florida following (Schlenker and Roberts 2009), i.e., counties colored green in Figures A2-A4 rather than all counties east of the Rocky Mountains (colored green or blue in Figures A2-A4). Graphs display the CO_2 fertilization effect of an increase in CO_2 concentration by 1 ppm on aggregate yields in the sample for corn, soybeans and wheat. The point estimates are marked by an x, and the 90% confidence intervals are added as lines. The bottom rows display the share of US production in the estimation sample.

Figure A15: Sensitivity Check: Accounting for Greenness Measures

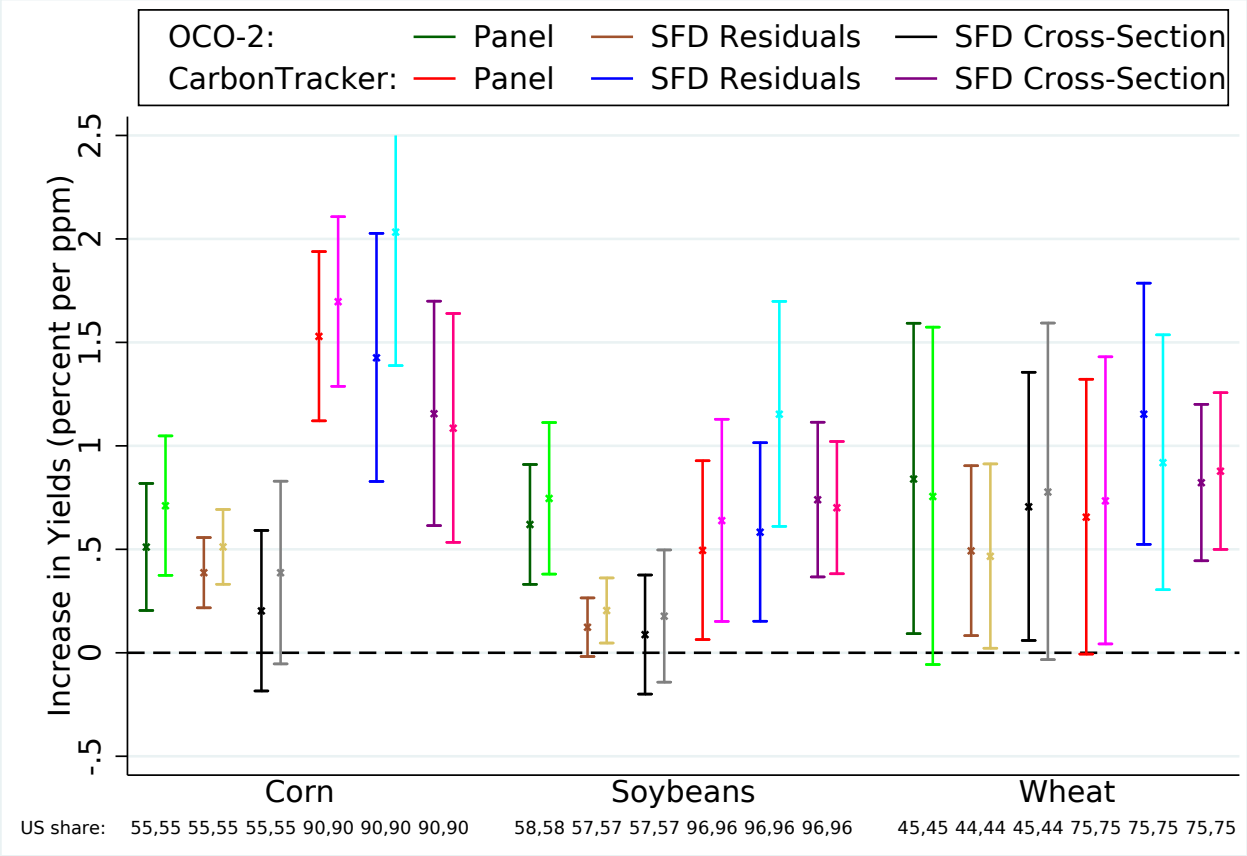

Notes: Figure replicates Figure 3 shown in darker colors for reference. The lighter colors rerun each specification (panel or spatial first difference using both the OCO-2 and CarbonTracker dataset), use a measure of greenness (solar-induced chlorophyll florescence (SIF) at 757nm in the case of OCO-2 and the Enhanced Vegetation Index (EVI) in the case of CarbonTracker) instead of the four weather variables. The greenness measure, like weather, should capture endogenous feedbacks, i.e., where more plant growth (higher greenness) reduces CO_2. Graphs display the CO_2 fertilization effect of an increase in CO_2 concentration by 1 ppm on aggregate yields in the sample for corn, soybeans and wheat. The point estimates are marked by an x, and the 90% confidence intervals are added as lines. The bottom rows display the share of US production in the estimation sample.

Figure A16: Sensitivity Check: Using CO_2 Readings from April-June Only

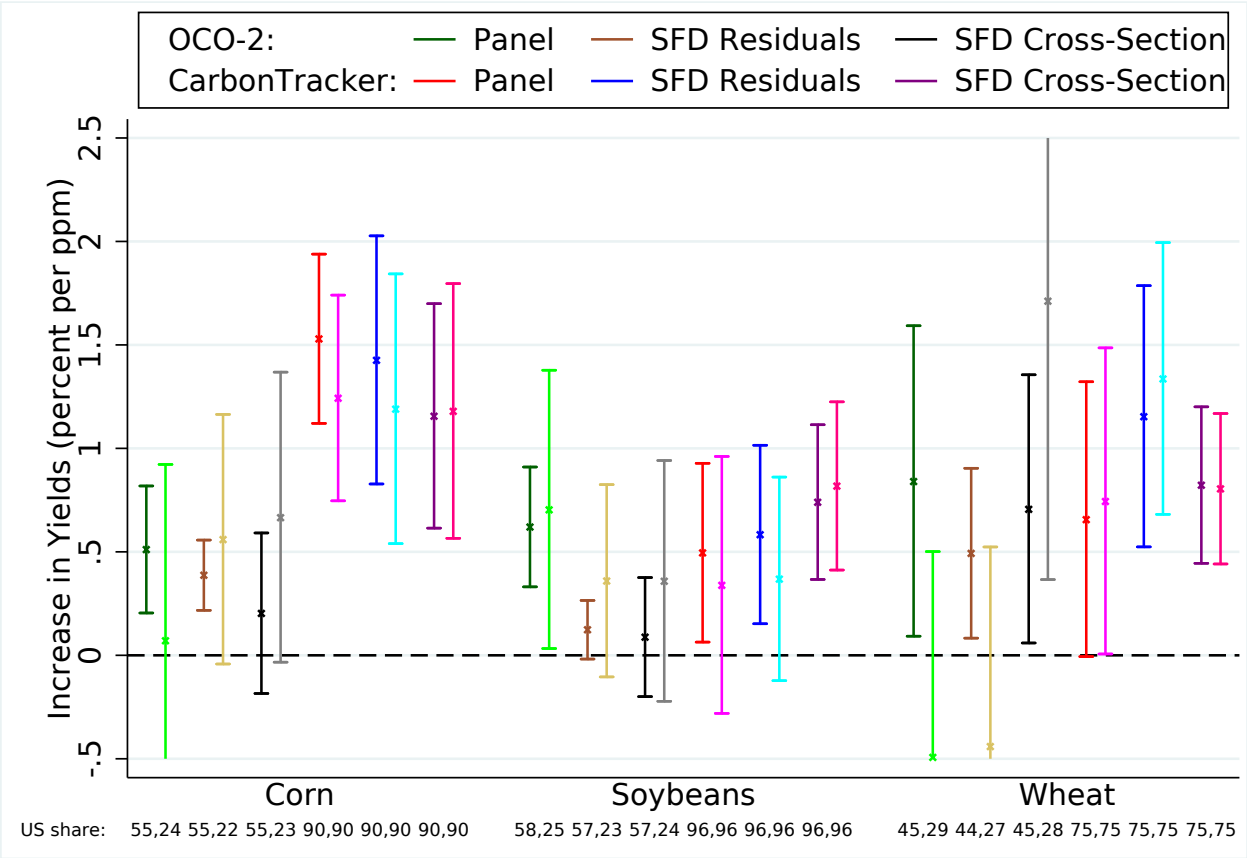

Notes: Figure replicates Figure 3 shown in darker colors for reference. The lighter colors rerun each specification (panel or spatial first difference (SFD) using both the OCO-2 and CarbonTracker dataset), but only include CO_2 readings for April-June rather than April-September. All other controls (weather and pollution variables) are still averaged over April-September. Graphs display the CO_2 fertilization effect of an increase in CO_2 concentration by 1 ppm on aggregate yields in the sample for corn, soybeans and wheat. The point estimates are marked by an x, and the 90% confidence intervals are added as lines. The bottom rows display the share of US production in the estimation sample.

Figure A17: Sensitivity Check: Not Accounting for Other Pollutants

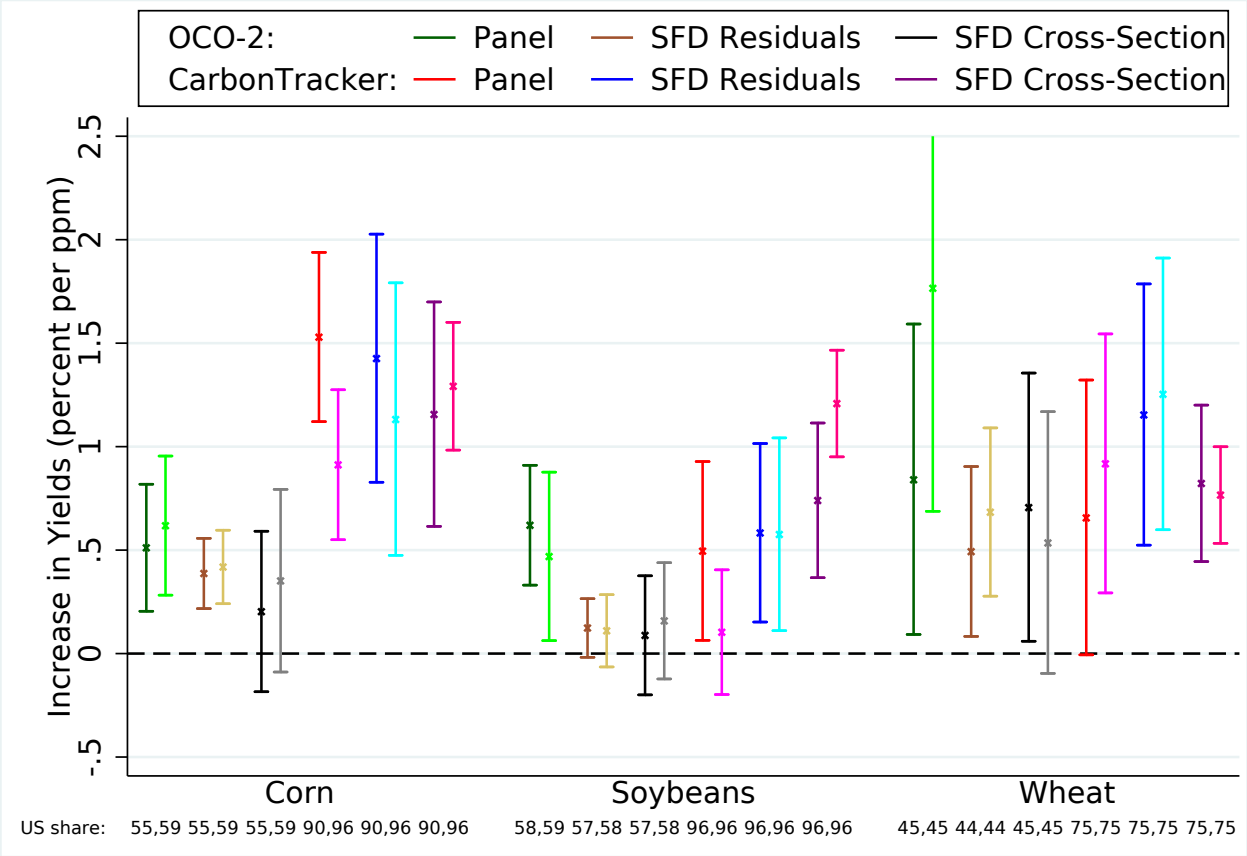

Notes: Figure replicates Figure 3 shown in darker colors for reference. The lighter colors rerun each specification (panel or spatial first difference (SFD) using both the OCO-2 and CarbonTracker dataset), but do not account for other co-pollutants (CO, NO_2, O_3, PM_{10}, SO_2). Graphs display the CO_2 fertilization effect of an increase in CO_2 concentration by 1 ppm on aggregate yields in the sample for corn, soybeans and wheat. The point estimates are marked by an x, and the 90% confidence intervals are added as lines. The bottom rows display the share of US production in the estimation sample.

Table A1: Effect of CO_2 on Log Yields with Urban Interaction

	Corn				Soybeans				Winter Wheat			
	(1a)	(1b)	(1c)	(1d)	(2a)	(2b)	(2c)	(2d)	(3a)	(3b)	(3c)	(3d)
CO2 x (urban = 1)	0.510***	-0.407	1.517***	0.642	0.618***	-3.280	0.494*	0.928	0.836*	3.185**	0.654	0.180
	(0.181)	(1.298)	(0.238)	(0.458)	(0.170)	(3.722)	(0.254)	(1.138)	(0.440)	(1.380)	(0.390)	(0.687)
CO2 x (urban = 2)		0.537		1.306***		0.490		0.469		0.438		0.677**
		(0.452)		(0.284)		(0.444)		(0.344)		(1.017)		(0.305)
CO2 x (urban = 3)		0.725*		1.437***		0.742		0.876**		-0.394		0.426
		(0.415)		(0.332)		(0.604)		(0.343)		(1.367)		(0.350)
CO2 x (urban = 4)		0.626		1.608***		0.396		0.121		-0.024		1.233**
		(0.619)		(0.292)		(0.346)		(0.310)		(0.799)		(0.500)
CO2 x (urban = 5)		0.659		1.643***		0.588		0.436		1.357*		0.877**
		(0.403)		(0.316)		(0.382)		(0.313)		(0.659)		(0.366)
CO2 x (urban = 6)		-0.542		1.531***		0.461		0.538**		0.959		0.432
		(0.368)		(0.271)		(0.358)		(0.217)		(1.302)		(0.503)
Moderate degree days (1000)	0.366***	0.230	0.234**	0.234**	0.459***	0.413***	0.525***	0.525***	0.301	0.358	-0.323***	-0.323***
	(0.100)	(0.206)	(0.085)	(0.085)	(0.102)	(0.138)	(0.074)	(0.074)	(0.233)	(0.380)	(0.070)	(0.070)
Extreme degree days (100)	-0.319***	-0.332***	-0.313***	-0.314***	-0.453***	-0.450***	-0.525***	-0.524***	0.011	-0.010	-0.014	-0.014
	(0.056)	(0.084)	(0.064)	(0.063)	(0.087)	(0.093)	(0.050)	(0.050)	(0.208)	(0.184)	(0.027)	(0.027)
Precipitation (m)	0.373	0.463	0.673***	0.673***	0.299	0.366	1.227***	1.228***	1.367**	1.377*	1.123***	1.127***
	(0.263)	(0.317)	(0.153)	(0.152)	(0.296)	(0.462)	(0.189)	(0.190)	(0.485)	(0.705)	(0.162)	(0.166)
Precipitation Squared	-0.285*	-0.365*	-0.471***	-0.470***	-0.252	-0.312	-0.782***	-0.783***	-1.210***	-1.273**	-0.976***	-0.979***
	(0.161)	(0.198)	(0.121)	(0.120)	(0.206)	(0.317)	(0.118)	(0.119)	(0.349)	(0.501)	(0.120)	(0.123)
CO (daily mean)	-4.719	-4.508	0.468	0.466	-3.190	-2.142	0.202	0.218	-5.931	-1.583	-0.011	-0.004
	(2.798)	(3.560)	(0.625)	(0.621)	(4.124)	(3.879)	(0.681)	(0.679)	(5.818)	(6.180)	(0.705)	(0.706)
NO2 (daily mean)	-3.714**	-3.999*	0.529	0.551	-2.723	-4.040	-0.066	-0.066	1.243	-0.667	1.089**	1.086**
	(1.717)	(2.072)	(0.427)	(0.421)	(2.408)	(2.634)	(0.543)	(0.550)	(2.814)	(3.532)	(0.513)	(0.501)
PM10 (daily mean)	-0.408	-0.358	-0.192	-0.188	-0.710*	-0.717	-0.283*	-0.279*	-2.483**	-2.033*	-0.958***	-0.964***
	(0.604)	(0.759)	(0.224)	(0.223)	(0.349)	(0.457)	(0.160)	(0.161)	(0.975)	(1.052)	(0.199)	(0.200)
SO2 (daily mean)	-0.996	-1.070	2.393*	2.372*	-1.709	-1.845	-1.665*	-1.685*	-1.933	-2.515	-0.457	-0.429
	(1.280)	(1.480)	(1.259)	(1.257)	(1.430)	(1.529)	(0.914)	(0.916)	(1.953)	(2.379)	(1.144)	(1.134)
O3 (1st spline variable)	-0.034***	-0.035**	-0.006	-0.006	-0.015	-0.016	0.001	0.001	-0.039	-0.049	-0.002	-0.002
	(0.010)	(0.014)	(0.008)	(0.008)	(0.012)	(0.014)	(0.007)	(0.007)	(0.028)	(0.041)	(0.008)	(0.008)
O3 (2nd spline variable)	0.307***	0.309**	0.017	0.018	0.070	0.070	-0.032	-0.032	0.254	0.329	-0.030	-0.031
	(0.102)	(0.143)	(0.079)	(0.079)	(0.120)	(0.136)	(0.071)	(0.071)	(0.295)	(0.423)	(0.096)	(0.096)
O3 (3rd spline variable)	-0.696**	-0.687*	0.051	0.046	-0.062	-0.040	0.115	0.116	-0.418	-0.567	0.124	0.125
	(0.256)	(0.363)	(0.198)	(0.199)	(0.300)	(0.341)	(0.171)	(0.170)	(0.763)	(1.069)	(0.253)	(0.253)
O3 (4th spline variable)	0.538*	0.463	-0.319	-0.314	-0.220	-0.308	-0.194	-0.196	-0.090	-0.012	-0.179	-0.181
	(0.278)	(0.404)	(0.222)	(0.223)	(0.323)	(0.366)	(0.166)	(0.166)	(0.861)	(1.135)	(0.274)	(0.274)
O3 (5th spline variable)	-0.255	0.030	0.636**	0.633**	0.593*	0.788*	0.236	0.237	0.627	0.466	0.094	0.094
	(0.305)	(0.438)	(0.236)	(0.236)	(0.345)	(0.398)	(0.162)	(0.162)	(0.907)	(1.064)	(0.210)	(0.210)
O3 (6th spline variable)	0.375	-0.430	-0.848***	-0.845***	-0.699	-1.058	-0.299	-0.301	-0.719	0.571	-0.012	-0.010
	(0.565)	(0.505)	(0.261)	(0.262)	(0.569)	(0.691)	(0.197)	(0.198)	(1.368)	(1.396)	(0.175)	(0.176)
R-squared	0.8962	0.9075	0.7439	0.7439	0.8933	0.9074	0.7613	0.7614	0.8910	0.9019	0.7694	0.7695
Observations	4316	3480	29298	29298	4127	3374	26932	26932	2658	2174	23419	23419
CO_2 data	OCO-2	CT	OCO-2	CT	OCO-2	CT	OCO-2	CT	OCO-2	CT	OCO-2	CT

Notes: Tables regresses log yields on CO_2, four weather variables, and five pollution variables. Columns (a) and (c) are the panel results shown in Figure 3 using OCO-2 and CarbonTracker data, respectively. Columns (b) and (d) interact CO_2 with the six categories of urban extent from USDA. All columns include county fixed effects and county specific time trends as the variable shave been trending upward over time (see Figure A5 for discussion). Errors are clustered at the state level. Stars indicate significance levels: * 10%, ** 5%, *** 1%.

Table A2: Effect of GDP Growth on Log Yields

	Corn		Soybeans		Winter Wheat	
	(1a)	(1b)	(2a)	(2b)	(3a)	(3b)
GDP Growth Rate	0.549	0.389	-0.038	-0.024	-0.061	-0.191
	(0.847)	(0.513)	(0.397)	(0.382)	(0.828)	(0.545)
Time (x100)	2.099***	3.858***	1.254***	1.099***	1.356***	2.791***
	(0.083)	(0.247)	(0.040)	(0.174)	(0.082)	(0.222)
Time (x100) Squared		-2.416***		0.212		-1.971***
		(0.327)		(0.221)		(0.288)
R-squared	0.9104	0.9526	0.9350	0.9359	0.8663	0.9292
Observations	72	72	72	72	72	72

Notes: Tables regresses aggregate US log yields on GDP growth rates (change in log GDP). Columns (1a)-(1b) give the results for corn, (2a)-(2b) for soybeans, and (3a)-(3b) for wheat. Columns (a) include a linear time trend (years since 1947), while columns (b) also include a quadratic of the time trend. Stars indicate significance levels: * 10%, ** 5%, *** 1%.